


Ferulic Acid Methyl Ester Attenuates Cerebral Ischemia-Reperfusion Injury in Rats by Modulating PI3K/HIF-1 α /VEGF Signaling Pathway

Peijie Zhou*, Shangshang Yu*, Xuan Wang*, Xiaofei Zhang, Dongyan Guo, Chongbo Zhao, Jiangxue Cheng, Jing Wang, Jing Sun 

Department of Pharmaceutics, College of Pharmacy, The Key Laboratory of Basic and New Drug Research of Traditional Chinese Medicine, Shaanxi Provincial Engineering Technology Research Center for Traditional Chinese Medicine Decoction Pieces, Shaanxi University of Chinese Medicine, Xiayang, Shaanxi, People's Republic of China

*These authors contributed equally to this work

Correspondence: Jing Sun, Email ph.175@163.com

Background: Cerebral ischaemia-reperfusion injury (CIRI) could worsen the inflammatory response and oxidative stress in brain tissue. According to previous studies, ferulic acid methyl ester (FAME), as the extract with the strongest comprehensive activity in the traditional Chinese medicine Huang Hua oil dot herb, has significant anti-oxidative stress and neuroprotective functions, and can effectively alleviate CIRI, but its mechanism of action is still unclear.

Methods: Firstly, the pharmacological effects of FAME were investigated by in vitro oxidative stress and inflammatory experiments. Secondly, evaluate the therapeutic effects of FAME in the treatment of CIRI by brain histopathological staining and cerebral infarct area by replicating the in vivo MACO model. Thirdly, RNA-Seq and network pharmacology were utilized to predict the possible targets and mechanisms of FAME for CIRI at the molecular level. Finally, the expression of key target proteins, as well as the key regulatory relationships were verified by molecular docking visualization, Western Blotting and immunohistochemistry.

Results: The results of in vitro experiments concluded that FAME could significantly reduce the content of TNF- α , IL-1 β and ROS, inhibiting COX-2 and iNOS protein expression in cells ($p < 0.01$). FAME was demonstrated to have anti-oxidative stress and anti-inflammatory effects. The results of in vivo experiments showed that after the administration of FAME, the area of cerebral infarction in rats with CIRI was reduced, the content of Bcl-2 and VEGF was increased ($p < 0.05$). Network pharmacology and RNA-Seq showed that the alleviation of CIRI by FAME may be through PI3K-AKT and HIF-1 signaling pathway. Enhanced expression of HIF-1 α , VEGF, p-PI3K, p-AKT proteins in the brain tissues of rats in the FAME group was verified by molecular docking and Western Blotting.

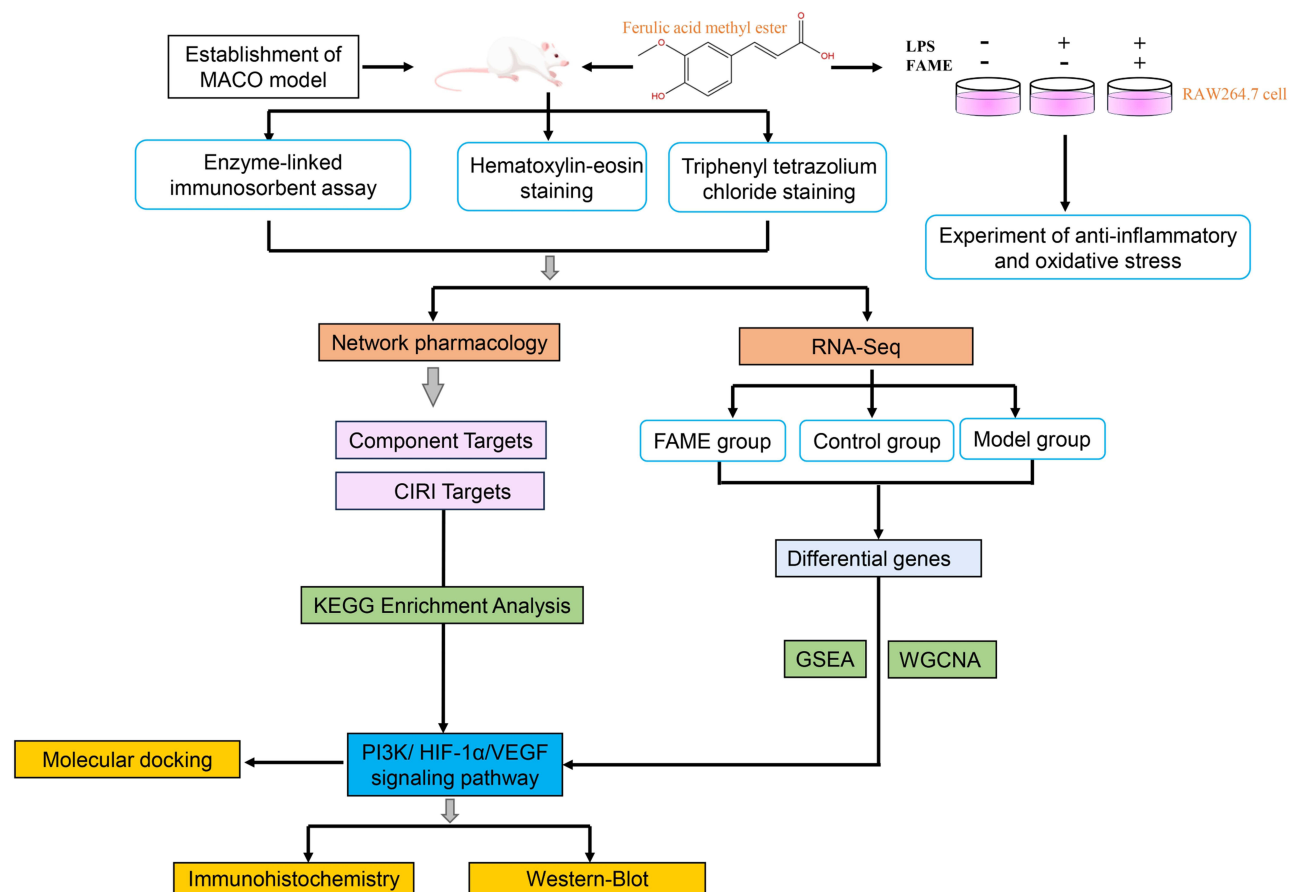
Conclusion: FAME possesses significant anti-inflammatory and anti-oxidative stress activities and alleviates CIRI through the PI3K/HIF-1 α /VEGF signaling pathway.

Keywords: ferulic acid methyl ester, cerebral ischemia-reperfusion injury, WGCNA, RNA-Seq, network pharmacology, molecular docking techniques

Introduction

Stroke, an acute cerebrovascular disease characterized by disruption of energy supply, neuronal death and brain tissue damage due to insufficient blood supply to the brain caused by rupture or blockage of blood vessels in the brain.¹ Ischemic stroke accounts for about 60% to 70% of all strokes,² has a higher incidence than hemorrhagic stroke, and is considered one of the most prevalent central nervous system (CNS) diseases.³ Clinical therapeutics for acute ischemic stroke mainly include two ways: arterial and venous thrombolysis and mechanical resection embolization. Among them, arterial thrombolysis and mechanical resection embolization have higher rates of restoring blood flow in cerebral arteries compared with intravenous thrombolysis.⁴ However, it is worth noting that cerebral ischemia-reperfusion injury (CIRI)

Graphical Abstract



can occur at any time, regardless of treatment, and is one of the risk factors secondary to essential perfusion therapy for ischemic stroke that needs to be urgently addressed.⁵ Currently, neurocytoprotective agent therapy is emerging as an emerging avenue for cerebral ischaemia-reperfusion injury. According to previous studies, the key targets include HIF-1A, Nrf2 and MPO, which effectively inhibit oxidative stress and inflammation in brain tissues through different mechanisms of action and alleviate the secondary damage of brain tissues caused by CIRI. Pathophysiological process of CIRI involves various mechanisms including oxidative stress, neuroinflammation, mitochondrial dysfunction,⁶ intracellular calcium overload and programmed cell death.⁷ These processes are interrelated and together lead to neuronal death, brain tissue damage and severe neurological deficits. Currently, drugs commonly used in the treatment of CIRI include free radical scavengers, excitatory amino acid antagonists, calcium channel blockers, and anti-inflammatory drugs.⁸ However, due to the complexity of CIRI mechanisms, single therapies usually fail to achieve the desired results, and new multi-targeted drugs will be viable therapeutic measures in the future.⁹

Ferulic acid methyl ester (FAME) was extracted from Huang Hua oil dot herb (*Tricyrtis maculata* (D. Don) J. F. Macbr). In the pre-research of the subject group, we found that Huang Hua oil dot herb exhibits favorable activating blood circulation to dissipate blood stasis, and is often used to treat ischemic cerebrovascular diseases. Our group therefore studied the chemical constituents isolated from Huang Hua oil dot herb and analyzed their effects on in vitro vasodilatation, in vitro anticoagulation, antioxidation, thrombolysis, and neurological function protection. We found that extracts of Huang Hua oil dot herb significantly, increased arterial and venous vessel diameter and values for blood flow velocity, improved blood microcirculation, and alleviated cellular peroxidative damage in hemorrhagic rats. Of the

isolated compounds, Ferulic acid methyl ester showed the most potent overall activity.¹⁰ In addition, ferulic acid methyl ester, as an ester derivative of ferulic acid, improves cellular uptake due to its special lipophilicity and has good permeability to the blood-brain barrier. According to the octanol–water partition coefficient measurements, the octanol–water partition coefficient of FAME was higher than that of FA. The ability of the cell to absorb the drug is largely determined by the lipophilicity of the drug and whether it can pass through the phospholipid bilayer.¹¹ It has been shown that, ferulic acid significantly promotes neuronal survival in the cerebral cortex only at a concentration of 200 mg/mL, whereas FAME significantly promotes neuronal survival in vitro at mass concentrations ranging from 0.16 to 20 mg/mL.¹² However, no study has elucidated the mechanism of action of ferulic acid methyl ester in the treatment of cerebral ischemia-reperfusion injury.

In this study, we induced ROS production in vitro and assayed the chemical activity of ferulic acid methyl ester. The MACO model was established in vivo to validate the pharmacodynamic effects of ferulic acid methyl ester on cerebral ischemia-reperfusion injury. And the key action targets were mined by using molecular docking visualization and RNA-Seq. We hope to be the first study to clearly elucidate the mechanism of action of ferulic acid methyl ester in the treatment of cerebral ischemia/reperfusion injury.

Materials and Methods

Materials and Reagents

Ferulic acid methyl ester with a purity of over 98%, was sourced from Shanghai yuanye Bio-Technology Co., Ltd. Mouse Mononuclear Macrophages Cells (Raw264.7) were Purchased from Wuhan Punuosai Life Science and Technology Co., Ltd. Assay kits for reactive oxygen species (ROS) was obtained from Nanjing Jianjian Biotechnology Co., Ltd., while ELISA kits for determining tumor necrosis factor- α (TNF- α), B-cell lymphoma-2 (Bcl-2), and Vascular endothelial growth factor (VEGF), were acquired from Jiangsu Meimian Industrial Co., Ltd. Kit for MTT was Purchased from Beijing Sole berg Technology Co., Ltd. Primary antibodies AKT and p-AKT were provided by Beijing Biosynthesis Biotechnology Co., Ltd. Antibodies for HIF1 α , VEGF, and β -actin was purchased from Proteintech Group, Inc., (Wuhan, China). PI3K and p-PI3k antibodies were sourced from Hangzhou HuaAn Biotechnology Co., Ltd., Horseradish peroxidase-conjugated secondary antibodies were obtained from Beyotime Biological Technology Co., Ltd., (Wuhan, China).

In Vitro Antioxidant Experiments

Establishment of Cell Culture and LPS-Induced Oxidative Stress Model

Raw264.7 Mouse Macrophages (Purchased from Wuhan Punuosai Life Science and Technology Co) were cultured in DMEM containing 10% FBS and 1% penicillin-streptomycin in a 5%, 37°C incubator.¹³ Cells in log phase were taken, density adjusted to 2×10^6 /mL, inoculated in complete medium, and cultured overnight in 96-well plates. The survival of RAW264.7 cells at different doses was determined according to the instructions of the MTT kit, and the absorbance was measured at 490 nm using an enzyme marker. The optimal dose of administration for cell survival was determined and then LPS was added 1 h after administration for oxidative stress model induction and placed in the incubator for 17 h.

Determination of Intracellular ROS

Intracellular ROS levels were quantified by DCF-DA fluorescence and measured according to the ROS kit operating instructions.¹⁴ Cells at a density of 2×10^6 /mL were inoculated in 96-well plates and preincubated with DCF-DA for 1 h at 37°C in the dark. After washing off the excess probe, the ROS content was measured under the fluorescence detection conditions of excitation wavelength 488 nm and emission wavelength 525 nm on a multifunctional enzyme marker.

Measurement of Classical Intracellular Indicators of Inflammation

The levels of TNF- α , IL-6 and NO in the cells were determined according to the ELISA kit instructions. Proteins were extracted from cells in the blank control, model, and FAME administration groups, and protein expression of COX-2 and iNOS was determined.

Validation of the Efficacy of Ferulic Acid Methyl Ester in the Treatment of CIRI

Ethics Statement

This study was approved by the Animal Ethics Committee of Shaanxi University of Traditional Chinese Medicine (SUCMDC20210901001). Moreover, experimental procedures were carried out in compliance with the Guide for Care and Use of Laboratory Animals (NIH publication, revised 1996).

Replication of the MCAO Model

SPF-grade adult male SD rats weighing approximately 260 g (animal license number SCXK [Chuan] 2020–030, from Chengdu Dashuo Experimental Animal Co., Ltd) were housed under standard conditions of temperature (25±2°C) and humidity (60±5) % for one week under adaptive conditions. Rats were fasted for 12 h prior to surgery. According to the requirements of blinded experiments for animal experiments in the Arrive 2.0 guidelines, all rats were randomly allocated to six groups: a sham-operated group; a model group; groups receiving low-dose (12.5 mg/kg), medium-dose (25.0 mg/kg), and high-dose Ferulic acid methyl ester (50.0 mg/kg); and a nimodipine (10.0 mg/kg) group, with 20 rats per group. Drug dosage selection based on pre-experimentation. The rats were pre-administered for 7 d before modeling and 20 were randomly selected for the sham-operated group before modeling, while the rest of the groups were modeled.

1.5% sodium pentobarbital was injected intraperitoneally into the rats to anesthetize them, and the MCAO model was established by producing a median cervical incision.¹⁵ After the vessels were separated, the common carotid and external carotid arteries were ligated; the internal carotid artery was temporarily clamped with an arterial clip, an incision was made in the vessel above the ligature point of the common carotid artery; and the vessel from the incision was inserted with a thread plug (MSRC35B200PK50) from the incision, tied with the pre-tied loose knot after insertion, and then sutured. After 2 h of ischemia, the wire embolus was carefully and uniformly withdrawn from the internal carotid artery of the rats to restore reperfusion for 24 h, after which appropriate iodophor was applied to prevent infection. The sham-operated group of rats underwent operations in an identical fashion except that the wire bolus was not inserted.

Neurological Deficit Evaluation and Determination of Brain-Tissue Water Content

After 24 h of reperfusion, the rats were scored behaviorally according to the Longa scale,¹⁶ and the scoring rules were as follows: 0 designated no neurologic deficit; 1 designated an inability to fully extend the front paw on the paralyzed side; 2 designated turning to the paralyzed side while walking; 3 designated leaning to the paralyzed side while walking; and 4 designated an inability to walk independently.

Five rats in each group were randomly selected for the determination of brain tissue water content, and after the behavioral scoring was finished the rats were euthanized by pentobarbital overdose, fresh brain tissue was taken from the rats, the surface of the brain was rinsed clean of blood using saline, the surface water was blotted on filter paper, the wet weight of the brain was weighed, and the brain tissue was heated in an oven at 105 °C for 72 h.¹⁷ The dry weight of the brain tissue was weighed after removal and the brain-tissue water content was calculated as Equation (1).

$$\text{Water content of brain tissue} = \frac{(\text{wet weight of brain tissue} - \text{dry weight of brain tissue}) \times 100\%}{\text{wet weight of brain tissue}} \quad (1)$$

Triphenyl Tetrazolium Chloride (TTC) Staining to Observe the Volume of Cerebral Infarction in Rats

After behavioral scoring the rats were euthanized as above. Fresh brain tissue was taken from the rats (the integrity of the brain was maintained as much as possible when taking samples), snap frozen in a -20 °C refrigerator for 20 min, removed and placed in a special brain-slicing mold, sliced at a 2 mm thickness (five slices total), and the slices placed in 2% TTC solution protected from light in a constant-temperature water bath at 37°C for 30 min. The brain sections were turned every 10 min to facilitate uniform staining and removed and fixed in 4% paraformaldehyde tissue fixative. Sections were photographed and the brain infarct volume was calculated using Image Pro Plus 6.0 software. White sections indicated the infarcted area.¹⁸

Determination of TNF- α , Bcl-2 and VEGF in Rat Serum Using Reagent Kits

After behavioral scoring, the rats were anesthetized, collected blood from the abdominal aorta, and the supernatant was centrifuged at 3000 r/min for 15 min at 4°C. The concentrations of TNF- α , Bcl-2 and VEGF in the serum were measured with assay kits (Purchased from Jiangsu Meimian Industrial Co., Ltd), and the absorbance values were determined with enzyme meter.¹⁹

Histopathologic Damage to Rat Brain as Observed by H&E Staining

Brain tissues were removed from the tissue fixative and paraffin sections were generated. Brains were sectioned at approximately 3 mm along the coronal plane, placed in pre-numbered embedding boxes, dehydrated for tissue transparency, soaked in paraffin for 3 h, and then the tissues were embedded in paraffin. After embedding, the brain tissues were placed in a low-temperature refrigerator for 10 min, and the embedded brain tissue was sectioned at 4 μ m, followed by stretching the brain sections in 75% ethanol with a soft brush.²⁰ The sections were then transferred to a distilled-water spreader at 42°C for complete stretching, removed with marked anti-detachment slides, allowed to dry naturally, and transferred to a thermostat at 65°C for 2 h. After drying, staining was conducted using a fully automated staining and the staining procedure was as described in the literature.²¹ We then placed the stained slides in a fully automated sealer, sealed the slides and cover slipped them for storage, placed the processed H&E-stained sections in a fully automated quantitative pathology imager, and ultimately photographed and analyzed them.

TUNEL Staining to Observe Apoptosis in Rat Brain Tissue Cells

Dewaxed paraffin sections were hydrated, treated with the TUNEL kit,²² and images were collected. Cells with positive TUNEL staining were observed under high magnification, and cells with brownish-yellow nuclei were considered apoptotic.

Network Pharmacology Analysis Prediction

Collection of the Targets of Ferulic Acid Methyl Ester Action and the Targets of CIRI

We obtained the SMILES number of Ferulic acid methyl ester by searching PubChem (<http://pubchem.ncbi.nlm.nih.gov>). And the target prediction was procured from the Swiss target prediction (<https://www.genecards.org/>) and MetatarFisher (<https://metatarget.scbdd.com/home/index/>) databases to predict the target sites of Ferulic acid methyl ester. The two parts of the data were then de-duplicated and integrated to obtain the full target site information for Ferulic acid methyl ester. The disease targets were collected and integrated from the GeneCards (<https://www.genecards.org>) and OMIM (<https://omim.org>) disease target databases. The intersection targets of drugs and diseases were mapped using the Venny 2.1.0 online mapping website to obtain the relevant therapeutic targets of Ferulic acid methyl ester in cerebral ischemia-reperfusion injury.²³

Network Construction and Analysis of Protein–Protein Interactions

The protein interaction network was constructed by the String database (<https://string-db.org/>), uploading the therapeutic targets to the database, setting the medium confidence to 0.400, and choosing to hide the free nodes to obtain the protein interaction network map.²⁴ The “drug-target-focus pathway” network was constructed with Cytoscape (3.7.2) software. The “dots” represent the drug components or targets, and the “lines” represent the interactions between the nodes. The greater the value of the target, the greater the role of the target in the network, and the more lines between the targets, the closer the connection between the targets.²⁵

Biofunction-Enrichment Analysis of Key Target Genes with GO and Enrichment Analysis with the KEGG Pathway

Enrichment analysis of the obtained intersection targets was conducted using Rstudio (Cluster Profiler package)²⁶ for GO biofunctional-enrichment analysis and an enrichment analysis of KEGG pathways. And the important biological processes and pathways in the enrichment results were briefly analyzed. The analysis was performed to uncover the potential mechanism(s) of action of Ferulic acid methyl ester in the treatment of cerebral ischemia-reperfusion injury.²⁷

RNA-Seq Analysis

Based on preliminary pharmacodynamic evaluation experiments. Brain tissue samples were randomly selected from 6 rats in each of the sham, model and FAME-administered groups for RNA-Seq analysis studies. The whole rat brains were snap frozen in liquid nitrogen and quickly transferred to a -80°C freezer for storage.²⁸

Total RNA was first extracted from rat brain tissue, and Trizol reagent maintained the integrity of RNA during cell fragmentation and lysis. Next, mRNA was isolated, fragmented, and primed, and the first and second strands and end fragments of cDNAs were synthesized in a PCR instrument to construct a transcriptomic library.²⁹ Finally, an RNA quality check was performed with an Agilent 2100 assay, and the quality of the RNA was determined by RNA integrity number using a 2100 instrument. RNA integrity number is a direct response to the quality of RNA, and a larger value indicates better and more complete RNA. The library construction and sequences were performed by Gene Denovo Biotechnology (Guangzhou, China). Analysis of differential gene expression before and after treatment of cerebral ischemia-reperfusion injury with ferulic acid methyl ester and differential gene function enrichment.

Uncovering Hub Genes in the Mechanism of Action of MF in the Treatment of CIRI by WGCNA Analysis

WGCNA was divided into two parts: expression clustering analysis and phenotype association, which mainly included four steps: correlation coefficient calculation between genes, identification of gene modules, co-expression network, and module-trait association.

First, the RNA-Seq data of ferulic acid methyl ester for cerebral ischemia-reperfusion injury as well as the trait files were imported into R language using the WGCNA (v1.47) software package,³⁰ and the genes were screened according to the TOM values. The weight coefficients of β were determined according to the principle of scale-free network, and the gene clustering tree was constructed using the gene co-expression profiles and the correlation of inter-gene expression. Modules were merged with the threshold of module eigenvalue similarity greater than 0.8, and the minimum number of genes in a module was set to 50.

Next, the modules obtained from the WGCNA analysis were analyzed for functional enrichment. And after, selected gene modules are identified, a map of gene regulatory networks in the modules are established by the degree of association between modules and traits and the enrichment of genes in the modules, and hub genes and specific types of genes (eg, transcription factors) are mined.³¹ Cytoscape 3.7.2 software was used to draw the co-expression network. Plot the top 100 relationship pairs of connectivity within the module by ranking the genes and genes in terms of weight value. Plot all relationship pairs for the top 10 most highly associated genes based on gene-module associations. Analyze the upstream and downstream regulatory relationships of hub genes through the above two gene network diagrams.³²

Molecular Docking

The positive control drug for the corresponding target was first searched from the DrugBank database (<https://go.drugbank.com/>), and the 3D structure of the core protein was next downloaded from the PDB (Protein Data Bank) (<http://www1.rcsb.org/>), followed by the 2D structure of Ferulic acid methyl ester, the positive drug and standard ligand from the Pubchem database as controls. Finally, molecular docking was performed using Discovery Studio 4.0 software in LibDock mode to obtain docking scores between Ferulic acid methyl ester and positive control drugs and targets, respectively.³³

Observation of the expression levels of HIF- α , Bcl-2, VEGF, and other proteins in brain tissues using immunohistochemistry (IHC)

Paraffin sections were dewaxed, hydrated, boiled in sodium citrate buffer for 15 min, inactivated in 3% H_2O_2 solution,³⁴ and treated with 3% bovine albumin at room temperature for 1 h. We added primary and secondary antibodies in a dropwise fashion, followed by the dropwise addition of an appropriate amount of peroxide-labeled streptavidin for color development and closed, and finally analyzed images using Image Pro Plus 6.0 software.

Detection of the Expression Levels of Key Proteins in Brain Tissue by Western Blotting (WB)

The frozen brain tissues were removed from a -80°C refrigerator, placed in labeled two-mL tubes in liquid nitrogen-insulated containers according to different groups, and then 500 μL of strong lysis solution was added (lysis solution preparation ratio, RIPA: PMSF=1000:1), the frozen brain tissues were subsequently removed, and approximately 50 mg of tissue was aliquoted from each group and placed in two-mL tubes.³⁵ The tissue fragments were homogenized with a grinder, the tubes placed into a pre-cooled (4°C) centrifuge for 10 min at 14,000 r/min, and the supernatant collected after centrifugation to obtain total tissue protein. According to the quantified protein concentration of each sample (using a BCA Protein Assay Kit), samples were prepared with an equal volume of RIPA and then added to the top of the protein-sample buffer, vortexed and mixed after centrifugation, placed into a 100°C water bath and heated for five min to denature the protein, and finally stored in a -80°C freezer for later use. The protein samples of each group were transferred to a PVDF membrane and electrophoresed using 10% SDS-PAGE. The membrane was then incubated overnight at 4°C with primary antibodies HIF1 α (proteintech, 66730-1-Ig, 1:5000), VEGF (proteintech, 19003-1-AP, 1:1000), β -actin (proteintech, 80455-1-RR, 1:5000), PI3K and p-PI3k (HUAbio, ET1608-70, Wuhan, Hubei, China), AKT and p-AKT antibodies (Bioss, bs-0061R, 1:5000). After three washes the membrane with TBST, added secondary antibody (1:10,000; Beyotime, P0258, Beijing, China), incubated the membrane at room temperature for 1 h, developed images with ECL luminescence reagent and then photographed the images. Image Pro Plus 6.0 analysis software was adopted to quantify the relative protein expression between groups of samples, with β -actin used as the internal reference protein.

Statistical Analysis

Data are expressed as means \pm standard deviation. We applied SPSS 19.0 for statistical analysis and executed one-way analysis of variance (ANOVA) to compare data among groups. $P < 0.05$ was considered statistically significant, and $p < 0.01$ was considered to be highly statistically significant.

Results

FAME Significantly Inhibits ROS Release

The induction of RAW264.7 cells by LPS was able to verify the anti-oxidative stress and anti-inflammatory activities of FAME, laying the foundation for the mechanism of action of FAME in the treatment of CIRI. According to the MTT results, the survival rate of cells was greater than 95% at $6\mu\text{M}$. Therefore, it can be considered that $6\mu\text{M}$ is the highest dose of Ferulic acid methyl ester to maintain the survival rate of RAW264.7 cells greater than 95%, as shown in [Figure 1A](#).

The antioxidant activity of Ferulic acid methyl ester was confirmed by measuring the intracellular ROS content at different administration concentrations by enzyme standardization. As fluorescence luminosity and the reactive oxygen species content was significantly reduced compared with that of the model group after LPS induction. Ferulic acid methyl ester could effectively inhibit the intracellular ROS production, as shown in [Figure 1B](#).

The levels of IL-6, TNF- α and NO in cell supernatants were determined according to ELISA kits. The results showed that the levels of IL-6, TNF- α and NO in cell supernatants were significantly reduced after FAME administration treatment ($P < 0.001$), as shown in [Figure 1C–E](#). In addition, the expression of COX-2 and iNOS proteins in the cells was significantly reduced by Western Blotting after FAME administration treatment, as shown in [Figure 1F–H](#). The above results suggest that FAME has oxidative stress inhibition and anti-inflammatory activities.

Ferulic Acid Methyl Ester Effectively Relieves CIRI

The structural formula of ferulic acid methyl ester is shown in [Figure 2A](#). After constructing the MACO model ([Figure 2B](#)), the water content of the brain tissue of the model rats was significantly increased ($P < 0.01$) ([Figure 2E](#)), indicating that the degree of brain edema in the model rats was more severe than that in the sham-operated group, and the cerebral edema scale of both the medium-dose group and the high-dose group was significantly reduced after

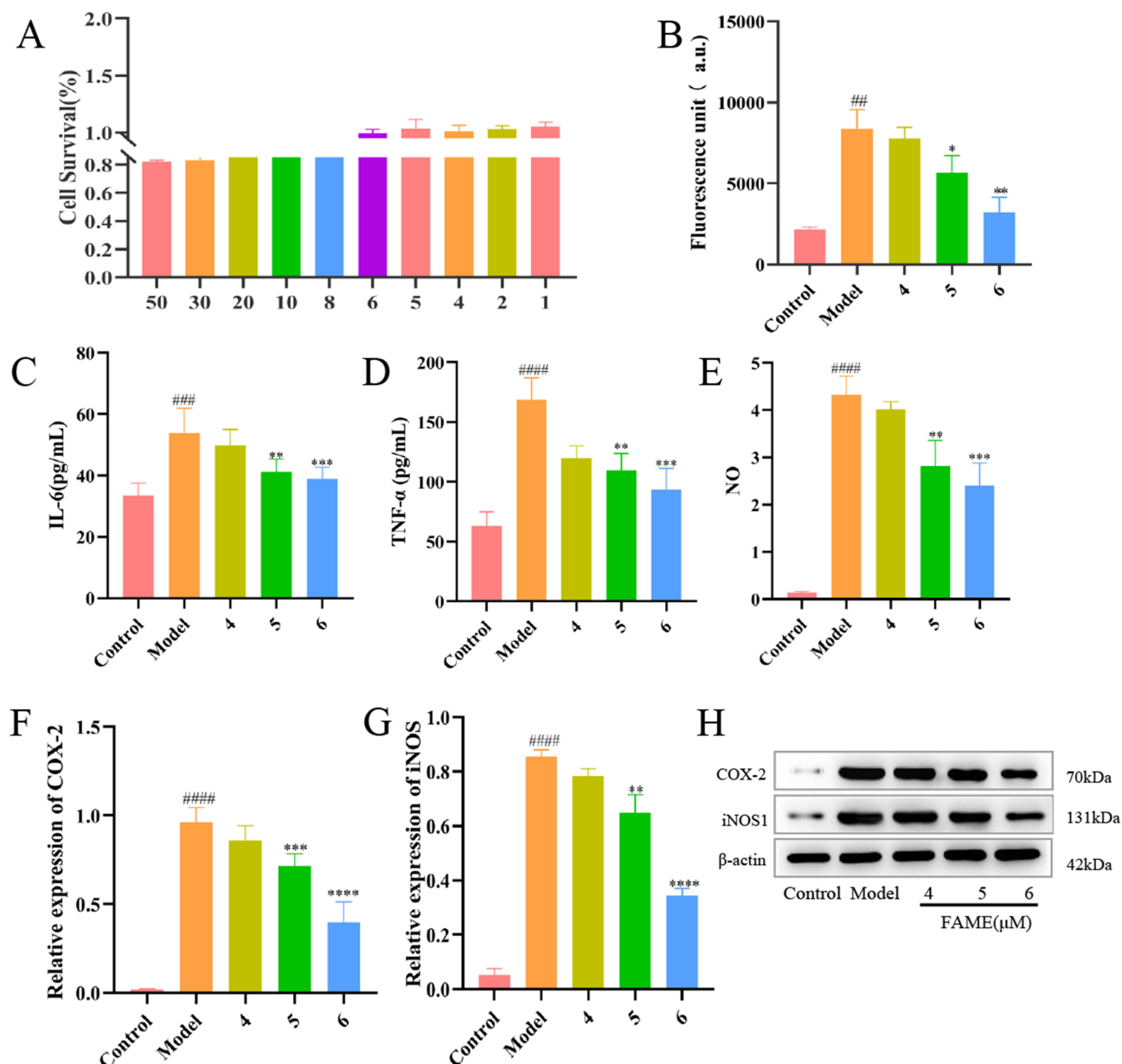


Figure 1 Results of in vitro antioxidant activity of FAME. (A) Cell survival rate at different concentrations. (B) Results of intracellular ROS content determination. (C) Results of intracellular IL-6 content determination. (D) Results of intracellular TNF- α content determination. (E) Results of intracellular NO content determination. (F) Intracellular COX-2 protein expression. (G) Intracellular iNOS protein expression. (H) Western blotting of intracellular COX-2 and iNOS proteins.

Notes: (Compared with the sham group ### $p < 0.01$, #### $p < 0.001$, ##### $p < 0.0001$; compared with the model group. * $p < 0.05$, ** $p < 0.01$, *** $p < 0.001$, **** $p < 0.0001$).

ferulic acid methyl ester administration ($P < 0.05$). According to the results of neurobehavioral scores, the rats in the sham-operated group showed no obvious signs of neurological damage, while the rats in the model group showed more obvious signs of neurological damage as shown in Figure 2D. The neurological scores of rats in the high-dose administration group were significantly reduced ($P < 0.01$), demonstrating that ferulic acid methyl ester was effective in reducing neurological damage in rats with cerebral ischemia. In addition, the results of TTC staining showed that the infarct area was significantly reduced with the increase of the administered dose, which indicated that pre-treatment of ferulic acid methyl ester significantly reduced the infarct volume after cerebral ischemia-reperfusion injury as shown in Figure 2C and F.

From the results of the assay ELISA kits we noted that after the administration of Ferulic acid methyl ester, the content of anti-apoptotic factors (Bcl-2) in cerebral ischemic rats rose significantly, promoting the expression of vascular

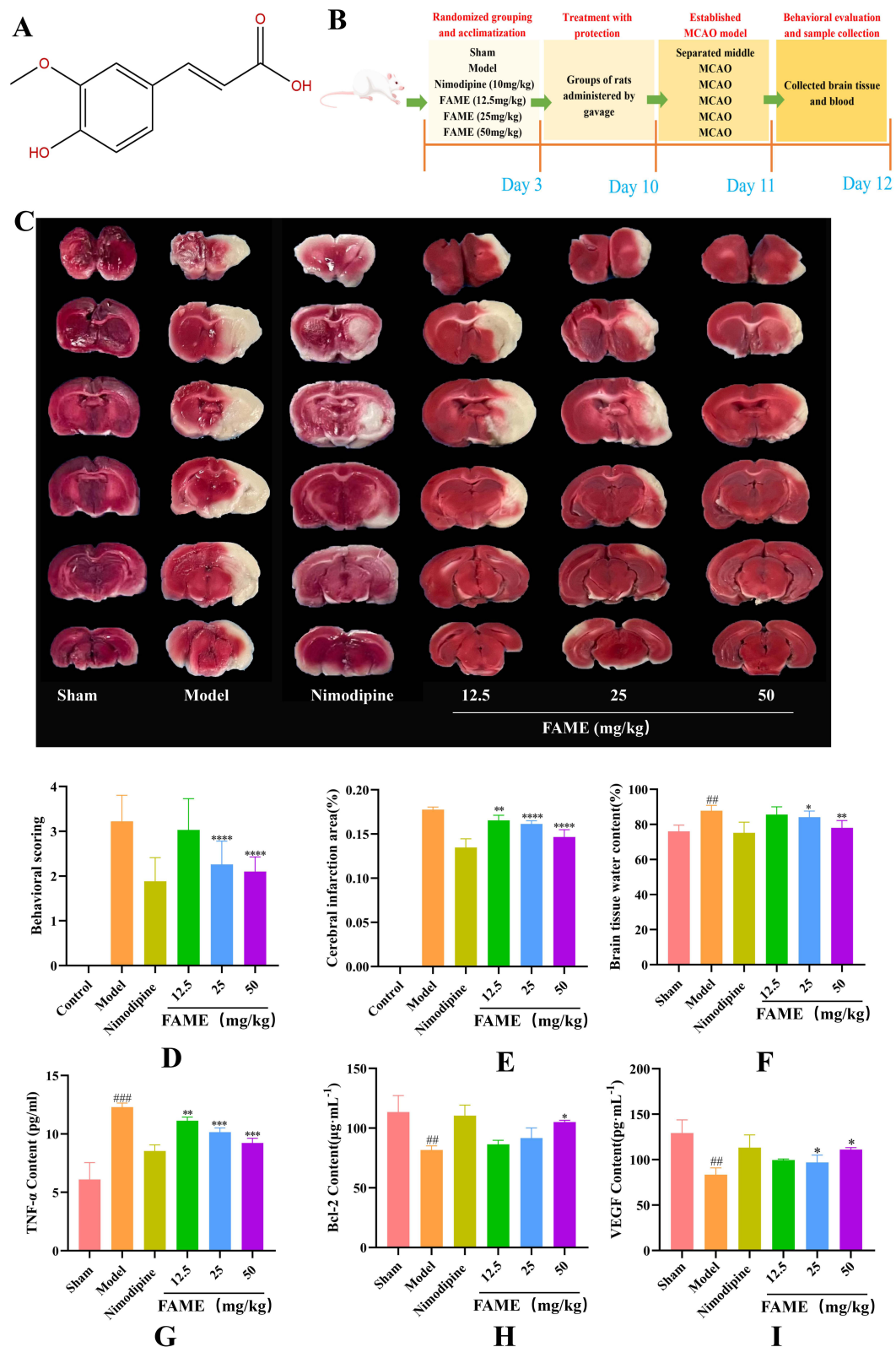


Figure 2 Therapeutic effects of FAME in CIRI rats. **(A)** Structural formula of ferulic acid methyl ester. **(B)** Therapeutic course of ferulic acid methyl ester in the treatment of cerebral ischemia-reperfusion injury. **(C)** TTC staining of rat brain tissue in each group (n=10). **(D)** Neurological deficit score of rats in each group (n=10). **(E)** Brain infarction area in each group (n=10). **(F)** The water content of brain tissues in each group (n=10). **(G)** levels of TNF-α in serum (n=10). **(H)** levels of Bcl-2 in serum (n=10). **(I)** levels of VEGF in serum (n=10).
Notes: (Compared with the sham group ###p<0.01, ####p<0.001; compared with the model group. *p<0.05, **p<0.01, ***p<0.001, ****p<0.0001).

endothelial cells along with diminishing the content of inflammatory factors *in vivo*. We therefore hypothesize that Ferulic acid methyl ester reduced cerebral ischemic injury and exerted its pharmacologic activity via an anti-apoptotic action, promoting vascular endothelial cell regeneration and reducing inflammatory injury as shown in Figure 2G–I.

Analyze the results of HE staining of brain tissue. The cortical neurons of our normal rat brain tissues were abundant, evenly stained, neatly arranged, clearly stratified, and without obvious inflammation or obvious pathologic changes. However, the cortical brain tissues of model rats showed a large number of vacuoles in the cytoplasm of neurons as well as in the neuropil—manifesting a sponge-like appearance—and this was accompanied by neuronal death or absence (black arrows), a small number of proliferating astrokeratinocytes (blue arrows), and brain cell derangement. Compared with the model group, the cortical layer of brain tissue in the nimodipine group occasionally showed vacuolar degeneration and cytoplasmic loss (black arrows), and the degree of lesions was reduced in the low-, medium-, and high-dose groups. The degree of nucleus fixation was not obvious, with the medium- and low-dose groups showing a slight improvement,³⁶ as shown in Figure 3A.

In addition, detection of apoptosis by TUNEL staining of brain tissue the number of apoptotic cells in the brain tissue of rats in the model group was significantly increased as observed by brownish-yellow nuclei (black arrows) upon using panoramic scanning software, and apoptosis in the ischemic semi-dark zone of the rat brains was observed congruent with the literature.³⁷ The number of apoptotic cells with brownish-yellow nuclei (black arrows) in the model group was significantly increased compared with the sham-operated group, and apoptosis in each administration group was reduced to differing degrees compared with the model group; the number of apoptotic cells in the high-dose administration group was significantly reduced, as shown in Figure 3B.

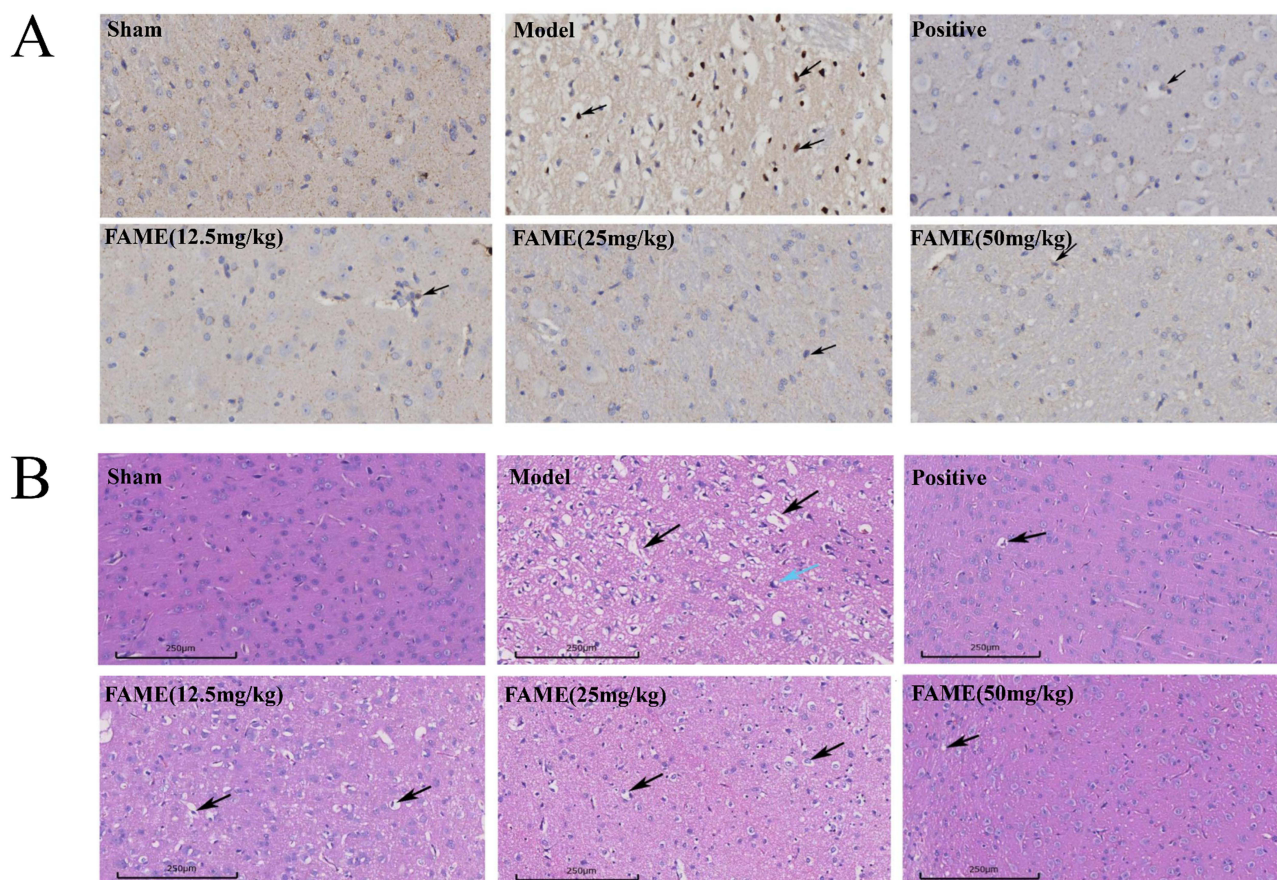


Figure 3 Brain histopathologic staining results. **(A)** Apoptosis of rat TUNEL stained brain cells in each group 40.00x. **(B)** HE staining results of rat brain tissue for each group 40.00x.

HIF-1 pathway may be an important mechanism of action of ferulic acid methyl ester in the treatment of cerebral ischemia-reperfusion injury

Identification of Component and Disease Targets and Construction of Network

The predicted targets of Ferulic acid methyl ester action from the two databases were aggregated to obtain 132 drug targets, while the targets obtained from the two disease databases were aggregated to obtain 1653 disease targets using Venny 2.1.0 for the intersection between drug and disease targets, so as to obtain 44 therapeutic targets, as shown in Figure 4A. A network of interactions between proteins diagram shows the interactions among the eight therapeutic targets. In the network diagram of topological analysis, the values of degree reflect the size and color of different nodes in the diagram, and the combined score represents the thickness of different lines in the diagram—the larger the combined score, the thicker the lines as shown in Figure 4B and D. The network diagram of “active ingredient-key target” constructed by the screening of key targets into Cytoscape 3.7.2 software showed that Ferulic acid methyl ester could be used to treat cerebral infarction through multi-target and multi-pathway synergistic actions, as shown in Figure 4C.

Results of Biological Function- and Pathway-Enrichment Analyses of Key Targets

A total of 1157 GO entries were identified using Rstudio software for GO biofunctional-enrichment analysis of the intersection targets, of which 1080 entries were for Biological Processes, mainly involving Regulation of inflammatory

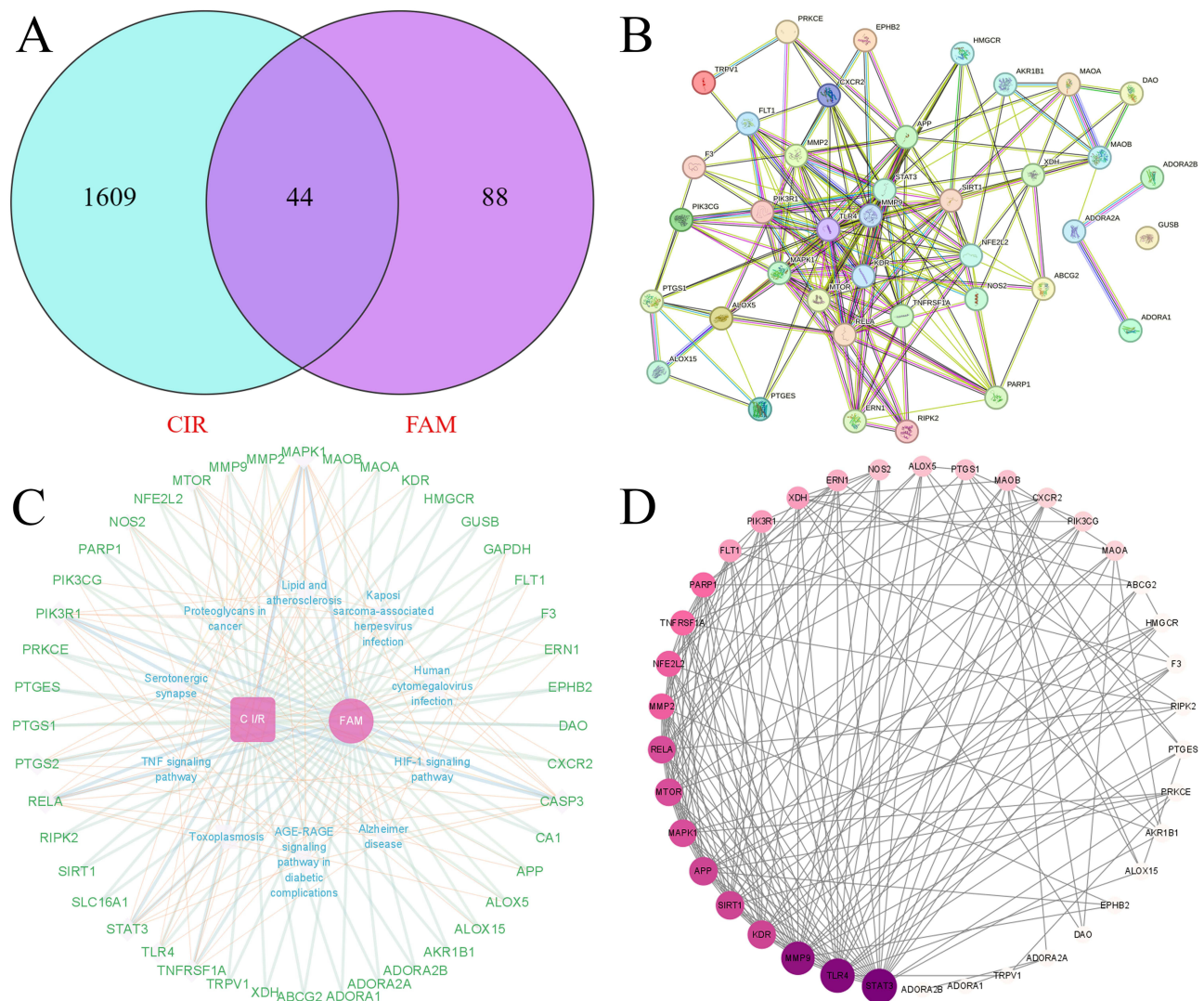


Figure 4 Constructed component disease interaction maps using network pharmacology approach. **(A)** Intersectional gene target map of Ferulic acid methyl ester and farcalic ischemia-reperfusion injury. **(B)** PPI network map. **(C)** Cytoscape network map. **(D)** PPI Degree Value Ranking.

response, Response to oxidative stress, Acute inflammatory response, and Reactive oxygen species biosynthetic process, as shown in Figure 5B. There were 48 entries for Cellular Components, including Nuclear envelope, Nuclear envelope lumen, Membrane raft, and Membrane microdomain, as shown in Figure 5C. Molecular Functions possessed 29 entries, including Oxidoreductase activity, acting on the CH-NH₂ group of donors, oxygen as acceptor, Oxidoreductase activity, acting on single donors with incorporation of molecular oxygen, incorporation of two atoms of oxygen, and Oxidoreductase activity, acting on single donors with incorporation of molecular oxygen, as shown in Figure 5D.

We conducted KEGG pathway-enrichment analysis on the intersection targets, and identified a total of 119 entries that principally involved HIF-1 signaling pathway, Serotonergic synapse, AGE-RAGE signaling pathway in diabetic complications, Lipid and atherosclerosis, TNF signaling pathway, Apoptosis, and Fluid shear stress and atherosclerosis. HIF-1 signaling pathway ranked first, indicating that the pharmacological effects of ferulic acid methyl ester in the treatment of cerebral ischemia/reperfusion injury are closely related to the expression of proteins on the HIF-1 pathway as well as gene regulation, as shown in Figure 5A.

Results of RNA-Seq Analysis of MF for CIRI

Principal Component Analysis (PCA) based on gene expression information using R language packages. As shown in Figure 6A, there is good dispersion between the groups of samples. When we compared the sequencing results of the sham-operated group, model group, and Ferulic acid methyl ester group, we identified 2476 genes as significantly differentially expressed, with 1218 up-regulated and 1259 down-regulated using as judgement criteria a false discovery rate < 0.05 and |log₂FC| > 1. The differential expression volcano map is shown in Figure 6D, and the differential gene heatmap between the model and sham-operated groups is shown in Figure 6B. Differential gene analysis veeny plots between groups are shown in Figure 6C.

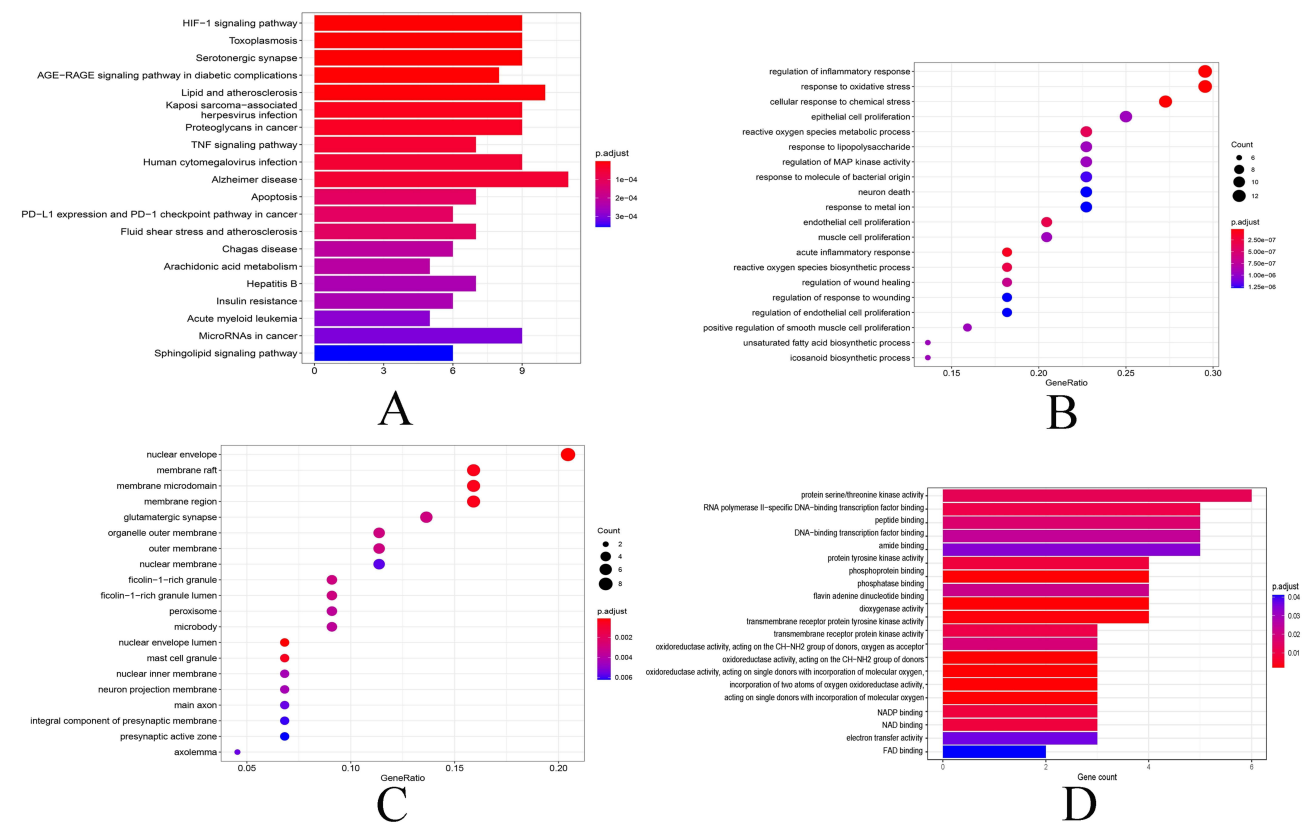


Figure 5 Network pharmacology enrichment to predict the possible mechanism of action of Ferulic acid methyl ester in the treatment of cerebral ischemia-reperfusion injury. (A) Top 20 pathway analysis based on the targets regulated by MA in CIRI. (B) Biological processes predicted by network pharmacology. (C) Cellular component predicted by network pharmacology. (D) Molecular function predicted by network pharmacology.

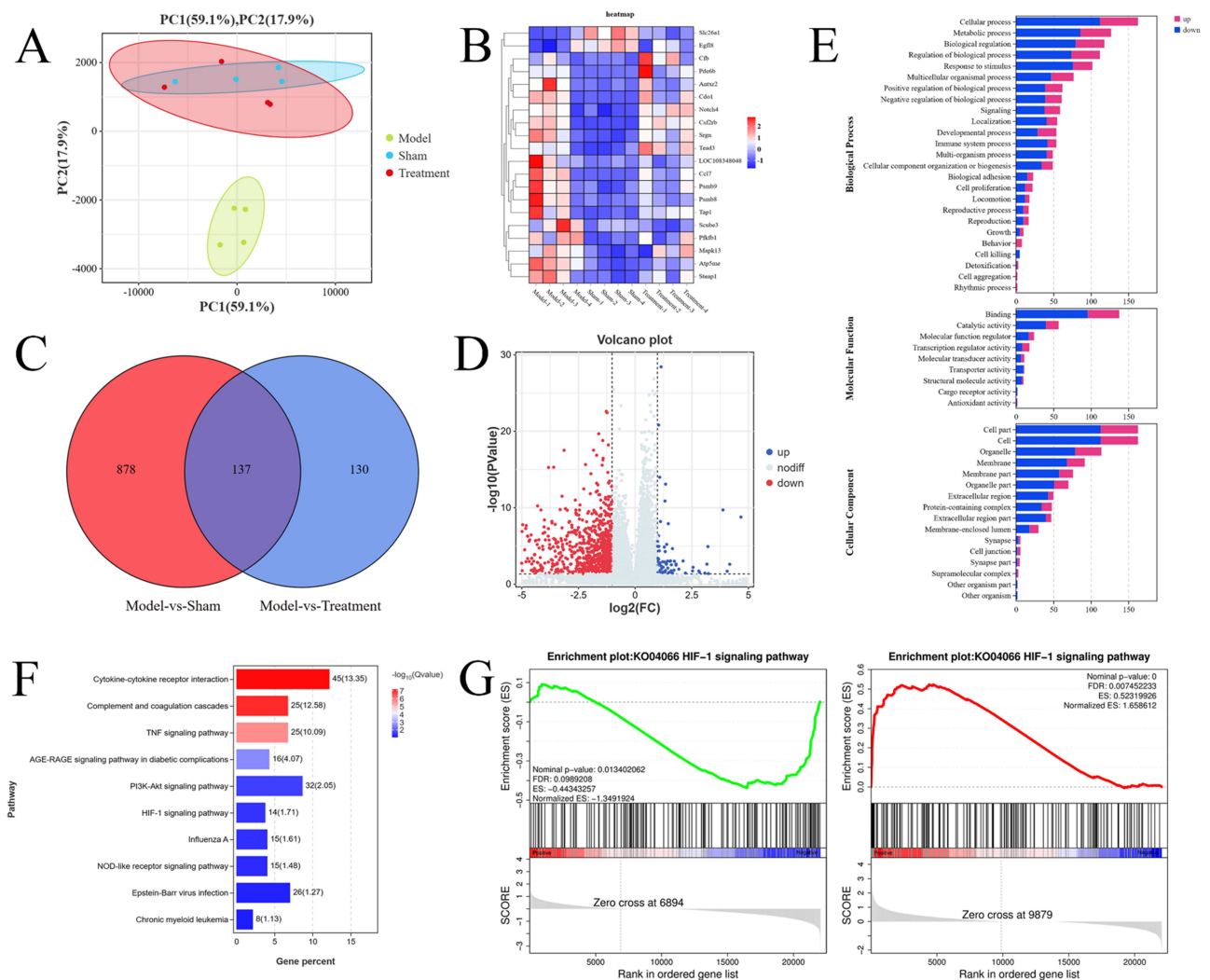


Figure 6 RNA-Seq enrichment results of FAME for CIRI. **(A)** Sample aggregation distribution map. **(B)** Heatmap of genes differentially expressed. Difference comparison volcano map **(C)**. Difference comparison volcano map. **(D)** Differential gene analysis veeny plots. **(E)** Results of differential gene GO enrichment based on RNA-Seq. **(F)** Results of differential gene KEGG enrichment based on RNA-Seq **(G)**. GSEA analysis of the HIF-1 signaling pathway.

In order to verify the key pathways and mechanisms underlying Ferulic acid methyl ester action in the treatment of cerebral ischemia-reperfusion injury as predicted by network pharmacology, we performed differential gene analysis of GO and KEGG pathway enrichments. A total of 333 KEGG pathways were enriched by differential expression of genes, including Complement and coagulation cascades, TNF signaling pathway, and MAPK signaling pathway. Of these, the possible pathways of action predicted by network pharmacology that approached HIF-1 ranked sixthly, as shown in Figure 6F. The differential gene GO enrichment included Cellular process, Biological regulation, Binding, and Cell part, as shown in Figure 6E.

In addition, Gene Set Enrichment Analysis (GSEA) was used to enrich the obtained differential expression data to obtain closely related genes and signaling pathways; the results showed that they mainly included TNF signaling pathway, p53 signaling pathway, PI3K-Akt signaling pathway, and VEGF signaling pathway. The presence of the HIF-1 pathway was again verified by GSEA-KEGG analysis as shown in Figure 6G.

Results of WGCNA Analysis

In this analysis, a total of 12540 genes were introduced and 10370 genes were retained by gene expression screening. The Power value was determined to be 8, so that the correlation coefficient between genes was greater than 0.8, as shown in

Figure 7A. The modules were combined according to the similarity of 0.6, and a minimum of 50 genes were set in each module to obtain the module eigengene and module hierarchy classification, as shown in **Figure 7B** and **E**. Modules were combined according to the similarity degree of 0.6, and at least 50 genes were set in each module to obtain the module characteristic genes and module hierarchical classification, as shown in **Figure 7C** and **D**. The analysis of the gene enrichment results in each module showed that the most genes were enriched in the brown module, as shown in **Figure 7G**. In the results of the association between each module and the trait files of cerebral ischemia-reperfusion injury, the brown module was significantly associated with the four trait files of Score, Area, TNF and VEGF, with a P value of less than 0.05, as shown in **Figure 7F**.

In addition, the gene regulatory network map based on the top 10 genes of MM in the brown module could be mined to show that HIF1A, PIK3R1 and STAT3 might be the Hub genes (highly associated genes) for the treatment of cerebral ischemia/reperfusion injury by ferulic acid methyl ester, among which PIK3R1 and STAT3 were highly correlated with the transcription factor HIF1A, which might be an important regulatory relationship. Trait and module MM-GS (correlation of expression of each gene with the module, MM; correlation of each gene with the trait, GS) analyses showed that HIF1A had high MM and GS values with the four traits, as shown in **Figure 7H**.

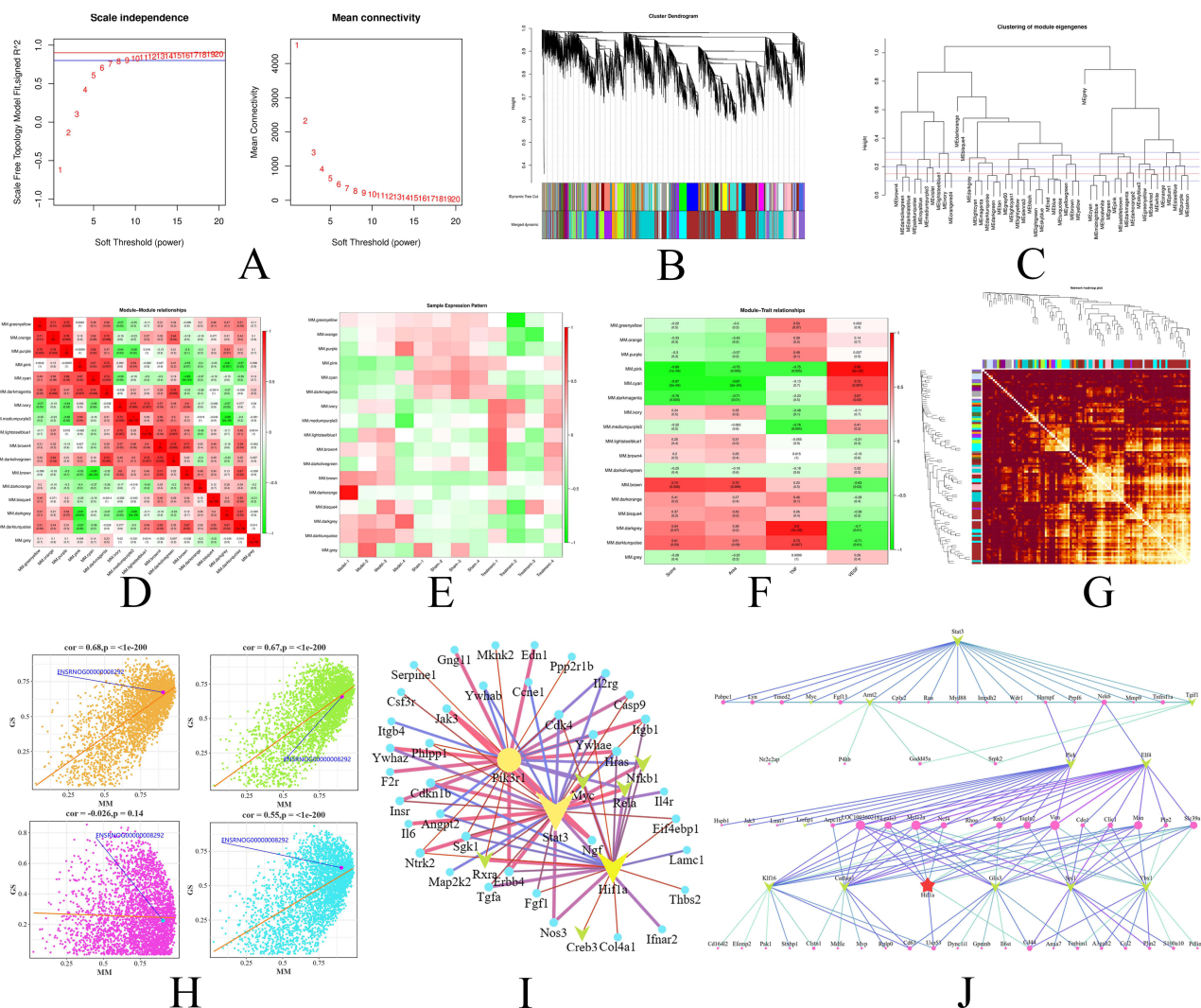


Figure 7 WGCNA results of FAME for CIRI. **(A)** The soft threshold was set at 8, where the blue horizontal line indicates the correlation coefficient 0.8 and the red horizontal line indicates the correlation coefficient 0.9. **(B)** module hierarchical clustering plot **(C)**. Module trait clustering plot **(D)**. Modules and inter-module correlation. **(E)** Samples and Modules correlation map. **(F)** trait association correlation map. **(G)** Gene enrichment correlation map for each module **(H)**. MM-GS Correlation Plot of Cerebral Infarct disease manifestation and Module Gene Association Analysis. **(I)** Gene regulatory network map between PIK3R1, STAT3 and HIF1A. **(J)** Network diagram of HIF-1A upstream and downstream regulatory relationships.

From the WGCNA gene regulatory network map, it can be seen that STAT3 is an important regulator upstream of HIF1A, and the transcription of STAT3 influences the transcription of downstream HIF1A. PIK3R1 and STAT3 are both regulatory proteins upstream of HIF1A, and with the transcriptional expression of PIK3R1 and STAT3, the expression of HIF1A is enhanced, as shown in [Figure 7I](#). In the top 10 gene regulatory network maps for gene-module association, HIF1A ranked high in abundance with PIK3R1 and STAT3, as shown in [Figure 7J](#).

Visual Validation of Molecular Docking of Hub-Gene

Using molecular docking to verify the binding activity between ferulic acid methyl ester and therapeutic targets, the target proteins were compared with the scores for Ferulic acid methyl ester and the positive control drug; we ascertained that Ferulic acid methyl ester showed better binding activity with both PIK3R1 and STAT3, suggesting that these may be key targets of Ferulic acid methyl ester activity against cerebral ischemia-reperfusion injury. For the study of standard ligands of 3D proteins, we performed PyMOL analysis. Both the standard ligand (1LT) and FAME interacted with amino acid residue VAL-851 in the protein PIK3R1 (7PG6) through hydrogen bonding, both the standard ligand (ATP) and FAME interacted with amino acid residue Ser-277 in the protein STAT3 (6GFA) through hydrogen bonding, both the standard ligand (X6K) and FAME interacted with amino acid residues TYR-2225 and VAL-2240 in the protein MTOR (4JT6) through hydrogen bonding, and both the standard ligand (DAO) and FAME interacted with amino acid residues TYR-2240 in the protein MTOR (5UCA) through hydrogen bonding. The standard ligand (DAO) and FAME both hydrogen-bond to PHE-53 and ASN-230 amino acid residues in the protein of TLR4, as shown in [Figure 8A–F](#) and [Table 1](#).

MF promotes HIF1 α protein expression through up-regulation of PI3K protein, thereby activating downstream VEGF production and alleviating CIRI

Immunohistochemistry and Western blotting of pathological tissues were able to clearly demonstrate the trend of relevant protein expression after FAME administration. Using immunohistochemistry, we noted that the expression level of HIF1 α was increased in the model group rats compared with the sham-operated group rats, and that it was also significantly elevated in each group administered FAME compared with the model group rats ($p < 0.05$). Relative to the sham-operated rats, the expression levels of PI3K and VEGF were significantly down-regulated in the model group after cerebral ischemia ($p < 0.05$), while their expression levels were significantly augmented in each group receiving Ferulic acid methyl ester compared with the model group rats ($p < 0.05$). After treatment with Ferulic acid methyl ester, the expression levels of PI3K and VEGF were significantly increased in all groups ($p < 0.05$), as shown in [Figure 9](#).

Determination of the expression of key target proteins in the brain tissues of rats in each group by Western blotting to study the mechanism of FAME for CIRI, as shown in [Figure 10A](#). Compared with rats in the sham-operated group, the expression level of HIF1 α was elevated in the model group rats after cerebral ischemia and its expression level was significantly elevated in the rats administered the high-dose of FAME compared with the model group ($p < 0.01$), while the level of HIF1 α in the brain tissue of rats in the sham-operated group remained at normal levels under normoxic conditions and its expression was not induced compared with rats in the sham group, as shown in [Figure 10C](#). Compared with the rats in the sham-operated group, the expression level of VEGF was significantly down-regulated after cerebral ischemia in the model group rats ($p < 0.05$), and the expression level of P-pi3k, P-AKT and VEGF in all groups of rats was increased to differing degrees after the administration of Ferulic acid methyl ester, as shown in [Figure 10D and E](#); The protein expression level of VEGF was increased in the group with medium dose of Ferulic acid methyl ester ($p < 0.05$), as shown in [Figure 10B](#).

Discussion

Ischemic stroke is one of the most important causes of neurological morbidity and mortality worldwide, but concomitant cerebral ischemia-reperfusion injury makes the clinical management of acute ischemic stroke more challenging.³⁸ In the present study, we found that ferulic acid methyl ester can be used as a new multi-target drug to treat cerebral ischemia-

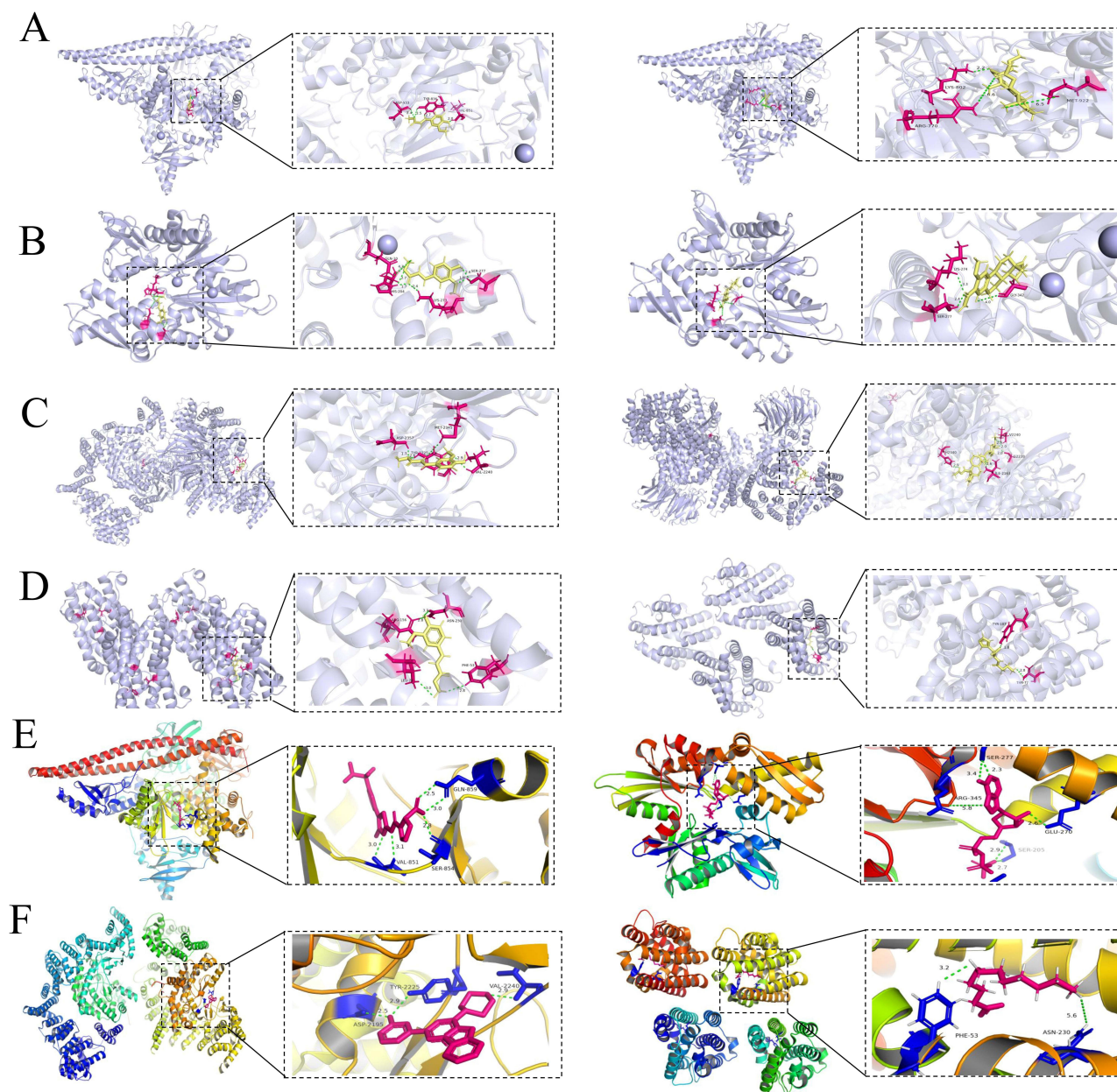


Figure 8 Molecular docking validation of Ferulic acid methyl ester. **(A)** The docking diagrams of protein PIK3R1 with FAME component (left) and Wortmannin positive drug (right). **(B)** The docking diagrams of protein STAT3 with FAME component(left) and Colforsin positive drug(right). **(C)** The docking diagrams of protein MTOR docking plot with FAME component(left) and Oleandrin positive drug(right). **(D)** The docking plot of protein TLR4 with FAME component(left) and Papain positive drug (right). **(E)** The docking plot of PIK3R1 with standard ligand ILT (left) and docking plot of STAT3 with standard ligand ATP (right). **(F)** The docking plot of MTOR with standard ligand X6K (left) and docking plot of TLR4 with standard ligand DAO (right).

reperfusion injury in three ways: attenuating oxidative stress injury, inhibiting neuroinflammation, and promoting cerebral angiogenesis.

Firstly, FAME significantly inhibited the ROS content produced by LPS-induced RAW264.7. The ROS content in the 6 μ M FAME administration group was significantly lower than that in the model group ($p < 0.01$). In addition, the expression of COX-2 and iNOS proteins was significantly reduced compared to the model, and the levels of two inflammatory factors, TNF- α and IL-6, were likewise significantly reduced ($P < 0.001$), in vitro experiment. Based on these results, it is concluded that FAME has a marked inhibitory effect on oxidative stress and anti-inflammatory activity. Oxidative stress plays a crucial pathophysiological role in the development of many CNS diseases. During CIRI,

Table I Molecular Docking Information of Key Target Proteins with FAME, Target-Positive Drugs, and Standard Ligand

No	Protein	PDB ID	Docking Compound	Combined Scores
1	PIK3R1	7PG6	FAME	83.098
			Wortmannin	101.266
			Standard ligand (ILT)	132.97
2	STAT3	6GFA	FAME	93.4584
			Colforsin	114.51
			Standard ligand (ATP)	140.332
3	MTOR	4JT6	FAME	83.098
			Oleandrin	90.072
			Standard ligand (X6K)	179.118
4	TLR4	5UCA	FAME	76.533
			Papain	85.9803
			Standard ligand (DAO)	125.764

overproduction of ROS leads to failure of the antioxidant system and ultimately induces oxidative stress. The reactive oxygen species (ROS) produced initiate excessive oxidative attack on essential cellular components that include DNA, lipids, and proteins.³⁹ ROS also induce programmed brain cell death and thus further enhance brain tissue damage.⁴⁰ An important regulator of oxygen homeostasis in the body is HIF1 α , known as hypoxia-inducible factor-1, is a dimer

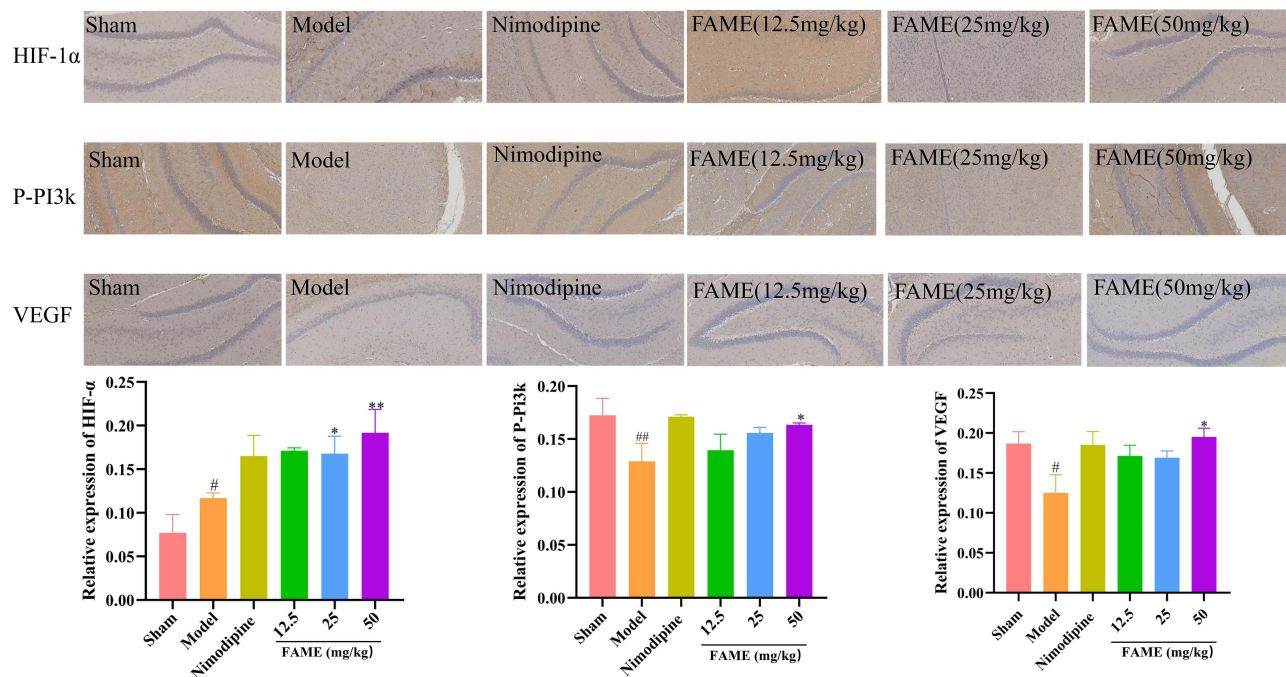


Figure 9 Immunohistochemical results of relevant factors in rat brain tissue after MACO model establishment.
Notes: (Compared with the sham group # $p < 0.05$, ## $p < 0.01$; compared with the model group. * $p < 0.05$, ** $p < 0.01$).

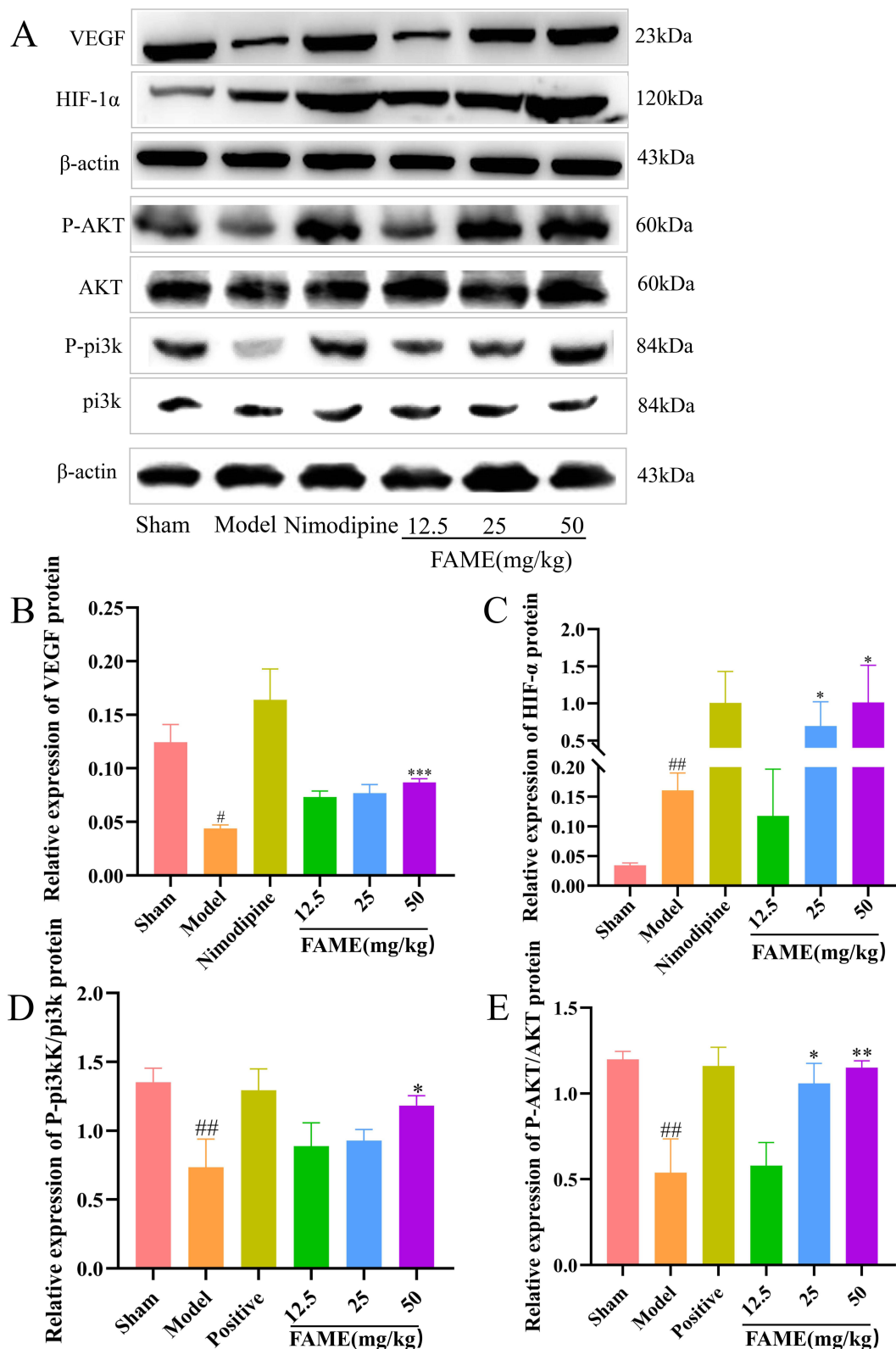


Figure 10 Western blot analysis of the expression levels of the relevant proteins in the brain tissue of each group of rats. **(A)** Western blotting of key target proteins in brain tissues of various groups of rats. **(B)** VEGF protein expression in brain tissue of rats in each group. **(C)** HIF-1 α protein expression in brain tissue of rats in each group. **(D)** P-PI3K/PI3K protein expression in brain tissue of rats in each group. **(E)** P-AKT/AKT protein expression in brain tissue of rats in each group. **Notes:** (Compared with the sham group [#] $p < 0.05$, ^{##} $p < 0.01$; compared with the model group. ^{*} $p < 0.05$, ^{**} $p < 0.01$, ^{***} $p < 0.001$).

composed of two subunits, α and β , of which the hypoxia-sensitive α subunit determines its biological activity and its expression level is closely related to various physiologic and pathologic processes in the body,⁴¹ with numerous studies showing that, HIF1 α is activated to participate in hypoxia-induced oxidative stress, when the brain is in a hypoxic state. It has been shown that HIF-1 reduces ROS production under hypoxic conditions possibly through a variety of complex pathways,⁴² including: subunit conversion of cytochrome c oxidase from COX4-1 to COX4-2 regulatory subunits, thereby increasing the efficiency of complex IV;⁴³ induction of pyruvate dehydrogenase kinase 1, which shunts pyruvate out of the mitochondria and induction of BNIP3, which triggers mitochondrial selective autophagy.⁴⁴ Among them, HIF-1 induces mitochondrial selective autophagy mechanism to reduce the production of reactive oxygen species has been demonstrated, LC3 (ATG8 in yeast) is a widely accepted marker of increased autophagy, and in the autophagic pathway,⁴⁵ HIF1 α promotes the formation of autophagosomes to induce mitochondrial selective autophagy, which is able to reduce ROS production from a major source in a hypoxic environment.⁴⁶ When we predicted by network pharmacology, we found that the primary mechanism of ferulic acid methyl ester in the treatment of cerebral ischemia-reperfusion injury is the HIF-1 signaling pathway. Transcriptome sequencing and GSEA analysis of differential genes before and after ferulic acid methyl ester treatment of cerebral ischemia-reperfusion injury revealed that the HIF-1 pathway was expressed in the same trend in the ferulic acid methyl ester administration group and the sham operation group. In addition, visualization of molecular docking results and protein immunoblotting of brain tissues from all MACO groups demonstrated that ferulic acid methyl ester activated the HIF-1 signaling pathway by upregulating the expression of HIF1 α and alleviated the oxidative stress injury brought about by cerebral ischemia and reperfusion.

Secondly, in the *in vivo* MACO model, the neurobehavioral scores of ferulic acid methyl ester administration showed that ferulic acid methyl ester could effectively reduce the neurological impairment. Results of ELISA kit showed that the TNF- α content of rat serum was significantly reduced, and the Bcl-2 content was significantly increased ($P < 0.001$). Inflammatory response is a subordinate chain reaction of oxidative stress in cerebral ischemia/reperfusion injury. And after cerebral ischemia/reperfusion, there is a significant increase in the expression of inflammatory cytokines in ischemic brain tissues, and inflammatory cytokines not only cause neurological damage, but also have neurotoxicity effects.⁴⁷ TNF- α not only causes cerebral edema and thrombosis by damaging vascular endothelial cells and altering permeability,⁴⁸ but also increases the adhesion of leukocytes and vascular endothelial cells through a variety of mechanisms, such as up-regulation of ICAM-1 and CD11/CD18, in addition to TNF- α interacting with endothelial cells leading to vascular dysfunction and coagulation processes.⁴⁹ Numerous studies have shown that ferulic acid methyl ester inhibits LPS-induced neuroinflammatory responses in human HMC3 microglia through the NF- κ B signaling pathway.⁵⁰ Ferulic acid methyl ester can inhibit neuroinflammation brought about by cerebral ischemia-reperfusion injury and has certain neuroprotective functions.

Thirdly, immunohistochemical staining and Western blotting of brain tissue showed up-regulation of P-pi3k, P-AKT and HIF1 α protein expression along with enhanced VEGF protein expression after ferulic acid methyl ester administration. Ferulic acid methyl ester activates downstream angiogenic pathways via HIF1 α . The PI3K/HIF1 α signaling pathway has been recognized to play an important role in neuroprotection and angiogenesis, as shown in [Figure 11](#). Scholars have shown that after intervention with the AKT-specific blocker wortmannin in a rat model of cerebral ischemia-reperfusion injury, the expression trend of its downstream regulator HIF- α is consistent with AKT,⁵¹ and in the present study, in which a MACO model was established to detect related protein expression, Ferulic acid methyl ester could upregulate the expression of the anti-apoptotic protein Bcl-2, demonstrating the role of PI3K/Akt survival pathway in the anti-apoptotic mechanism of Ferulic acid methyl ester treatment.⁵² Ferulic acid methyl ester activates downstream angiogenic pathways via HIF1 α . VEGF is a HIF- α downstream signaling factor that plays a crucial role in the early stages of angiogenesis, and selectively acts at VEGF receptors on endothelial cell membranes,⁵³ induces endothelial cell proliferation and migration, promotes vascular regeneration, and participates in angiogenesis during cerebral ischemia. In addition, some investigators have reported that VEGF ameliorates reperfusion injury in an organism by improving the collateral circulation. In this study, HIF1 α , PIK3R1 and STAT3 were pivotal genes in the mechanism of action of ferulic acid methyl ester in the treatment of cerebral ischemia/reperfusion injury according to WGCNA analysis, and HIF1 α received upstream regulation by PIK3R1 and STAT3. In addition, the data of this study provide some reference significance for the clinical treatment of CIRI, but it still has some limitations, and for the molecular docking of FAME with key target proteins, further in-depth validation by molecular dynamics simulation and other methods is needed in the future.

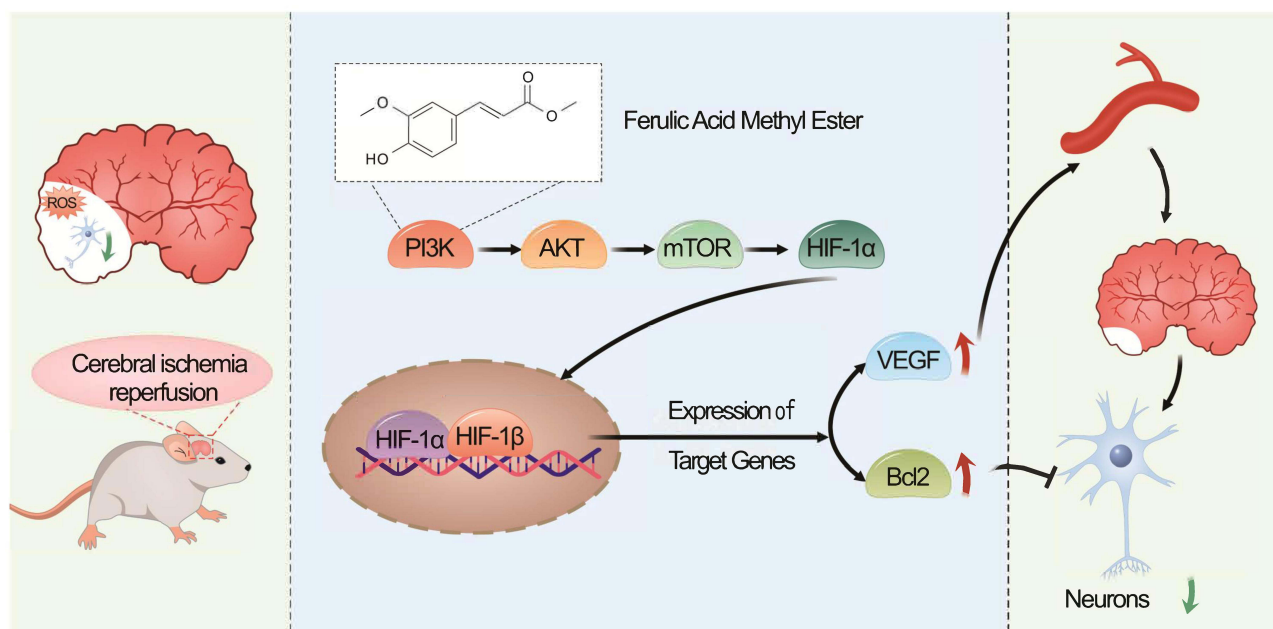


Figure 11 Mechanism of ferulic acid methyl ester as a novel target modulator of HIF-1 α to alleviate cerebral ischemia-reperfusion injury.

Conclusions

In summary, the study concluded that Ferulic acid methyl ester possesses antioxidant properties that enable it to effectively inhibit the production of reactive oxygen radicals and can be used as a natural antioxidant to treat cerebral ischemia-reperfusion injury caused by oxidative stress, and its mechanism of action may be through regulating the PI3K/HIF-1 α /VEGF signaling pathway, upregulating the expression of HIF1 α , Bcl2, and PI3K in a hypoxic environment reduce ROS production, inhibit oxidative stress and neuronal apoptosis, and activate downstream VEGF genes to promote regeneration of vascular endothelial cells.

Abbreviations

FAME, Ferulic acid methyl ester; CIRI, cerebral ischemia/reperfusion injury; ROS, reactive oxygen species; FBS, Fetal bovine serum; RNA-seq, RNA sequencing; PCA, Principal Component Analysis; WGCNA, Weighted gene correlation network analysis; HE, Hematoxylin and eosin; CIRI, Cerebral ischemia/reperfusion injury; TTC, 2,3,5-Triphenyltetrazolium chloride; CIRI, Cerebral ischemia/reperfusion injury; Bcl-2, B cell lymphoma -2; HIF-1, Hypoxia Inducible Factor-1; IHC, Immunohistochemistry; MCAO, Middle Cerebral Artery Occlusion; PPI, Protein Protein Interaction; VEGF, Vascular Endothelial Growth Factor; WB, Western Blot; TTC, 2,3,5-Triphenyl-2H-Tetrazolium Chloride; MTT, Methyl thiazolyl tetrazolium.

Acknowledgments

This study was supported by National Natural Science Foundation of China (82474054), National Key Research and Development Program of China (2021YFD1601004, 2023YFD1600402), Key R&D Program of Shaanxi Province (2024SF-ZDCYL-03-11), Xi'an Science and Technology Plan Project(20231H-JSJ0-0007), Shaanxi Provincial Administration of Traditional Chinese Medicine Project (2021-PY-005), Shaanxi Provincial High-level Key Discipline of Traditional Chinese Medicine - Chinese Medicine Concoctions, Shaanxi Provincial Engineering Technology Research Center for Chinese Medicine Beverage Tablets and Shaanxi Provincial University Engineering Technology Research Center for Aromatic Chinese Medicine Industry, Shaanxi Provincial University Youth Innovation Team for Key Technologies of Aromatic Chinese Medicine Industrialization.

Disclosure

The authors report no conflicts of interest in this work.

References

1. Zhao Y, Zhang X, Chen X, Wei Y, Li Y, Liu N. Neuronal injuries in cerebral infarction and ischemic stroke: from mechanisms to treatment (Review). *Int J Mol Med*. 2022;49(4):49. doi:10.3892/ijmm.2022.5104
2. Ajoalabady A, Wang S, Kroemer G, et al. Targeting autophagy in ischemic stroke: from molecular mechanisms to clinical therapeutics. *Pharmacol Ther*. 2021;225:107848. doi:10.1016/j.pharmthera.2021.107848
3. Xu S, Lu J, Shao A, Zhang JH, Zhang J. Glial Cells: role of the Immune Response in Ischemic Stroke. *Front Immunol*. 2020a;11:294. doi:10.3389/fimmu.2020.00294
4. Yang JL, Mukda S, Chen SD. Diverse roles of mitochondria in ischemic stroke. *Redox Biol*. 2018;16:263–275. doi:10.1016/j.redox.2018.03.002
5. Jurcau A, Ardelean IA. Molecular pathophysiological mechanisms of ischemia/reperfusion injuries after recanalization therapy for acute ischemic stroke. *J Integr Neurosci*. 2021;20:727–744.
6. Mo Y, Sun YY, Liu KY. Autophagy and inflammation in ischemic stroke. *Neural Regener Res*. 2020;15(8):1388–1396. doi:10.4103/1673-5374.274331
7. Tuo QZ, Zhang ST, Lei P. Mechanisms of neuronal cell death in ischemic stroke and their therapeutic implications. *Med Res Rev*. 2022;42(1):259–305. doi:10.1002/med.21817
8. Li M, Tang H, Li Z, Tang W. Emerging Treatment Strategies for Cerebral Ischemia-Reperfusion Injury. *Neuroscience*. 2022;507:112–124. doi:10.1016/j.neuroscience.2022.10.020
9. Xie Q, Li H, Lu D, et al. Neuroprotective Effect for Cerebral Ischemia by Natural Products: a Review. *Front Pharmacol*. 2021;12:607412. doi:10.3389/fphar.2021.607412
10. Ren L, Wang YZ, Zhang W, Sun Jet al.. Triculata A, a novel compound from *Tricyrtis maculata* (D. Don) J. F. Macbr. with biological properties. *Nat Prod Res*. 2021;35(21):3729–3737. doi:10.1080/14786419.2020.1736059
11. Botti G, Bianchi A, Pavan B, et al. Dalpiaz A Effects of Microencapsulated Ferulic Acid or Its Prodrug Ferulic acid methyl ester on Neuroinflammation Induced by Muramyl Dipeptide. *Int J Environ Res Public Health*. 2022;20(1):19. doi:10.3390/ijerph20010019
12. Sheng YM, Zhang J, Luo WZ, Zhang Y. Effect of ferulic acid and its esterified product on survival of rat cerebral cortex neurons cultured in vitro. *J Clin Rehabil Tissue Eng Res*. 2011;41:7730–7733.
13. Lv H, Ren H, Wang L, Chen W, Ci X. Lico A Enhances Nrf2-Mediated Defense Mechanisms against t-BHP-Induced Oxidative Stress and Cell Death via Akt and ERK Activation in RAW 264.7 Cells. *Oxid Med Cell Longev*. 2015;2015:709845. doi:10.1155/2015/709845
14. Zhang B, Zhai M, Li B, et al. Honokiol Ameliorates Myocardial Ischemia/Reperfusion Injury in Type 1 Diabetic Rats by Reducing Oxidative Stress and Apoptosis through Activating the SIRT1-Nrf2 Signaling Pathway. *Oxid Med Cell Longev*. 2018;2018(1):3159801. doi:10.1155/2018/3159801
15. Boys JA, Toledo AH, Anaya-Prado R, Lopez-Nebolina F, Toledo-Pereyra LH. Effects of dantrolene on ischemia-reperfusion injury in animal models: a review of outcomes in heart, brain, liver, and kidney. *J Invest Med*. 2010;58(7):875–882. doi:10.2310/JIM.0b013e3181e5d719
16. Longa EZ, Weinstein PR, Carlson S, Cummins R. Reversible middle cerebral artery occlusion without craniectomy in rats. *Stroke*. 1989;20(1):84–91. doi:10.1161/01.STR.20.1.84
17. Jiang HF, Guo YQ, Rehman FU, Jing L, Zhang JZ. Potential cerebrovascular protective functions of *Lycium barbarum* polysaccharide in alleviating hyperglycemia-aggravated cerebral ischemia/reperfusion injury in hyperglycemic rats. *Eur Rev Med Pharmacol Sci*. 2022;26(20):7379–7394. doi:10.26355/eurev_202210_30007
18. Cheng S, Chen C, Wang L. Gelsemine Exerts Neuroprotective Effects on Neonatal Mice with Hypoxic-Ischemic Brain Injury by Suppressing Inflammation and Oxidative Stress via Nrf2/HO-1 Pathway. *Neurochem Res*. 2023;48(5):1305–1319. doi:10.1007/s11064-022-03815-6
19. Ahmed MA, El Morsy EM, Ahmed AA. Pomegranate extract protects against cerebral ischemia/reperfusion injury and preserves brain DNA integrity in rats. *Life Sci*. 2014;110(2):61–69. doi:10.1016/j.lfs.2014.06.023
20. Barreto-Arce LJ, Kim HA, Chan ST, et al. Protection against brain injury after ischemic stroke by intravenous human amnion epithelial cells in combination with tissue plasminogen activator. *Front Neurosci*. 2023;17:1157236.
21. Buch P, Sharma T, Airao V, et al. Geraniol protects hippocampal CA1 neurons and improves functional outcomes in global model of stroke in rats. *Chem Biol Drug Des*. 2023;102(3):523–535. doi:10.1111/cbdd.14260
22. Xu X, Gao W, Li L, et al. Annexin A1 protects against cerebral ischemia-reperfusion injury by modulating microglia/macrophage polarization via FPR2/ALX-dependent AMPK-mTOR pathway. *J Neuroinflammation*. 2021;18(1):119. doi:10.1186/s12974-021-02174-3
23. Liu N, Jiang YY, Huang TT, Hou JC, Liu JX. A network pharmacology approach to explore mechanisms of Buyang Huanwu decoction for treatment of cerebral infarction. *Zhongguo Zhong yao za zhi. China J Chinese Materia Medica*. 2018;43(11):2190–2198. doi:10.19540/j.cnki.cjcmm.20180418.001
24. Song FJ, Fan B, Sun J. Explore compatibility mechanism of Xingnaojing injection in treating cerebral infarction based on network pharmacology. *Zhongguo Zhong yao za zhi. China J Chinese Materia Medica*. 2018;43(7):1366–1372. doi:10.19540/j.cnki.cjcmm.20180115.011
25. Wang X et al. (2023). Cinnamon essential oil based on NLRP3 inflammasome and renal uric acid transporters for hyperuricemia. *Food Bioscience*, 56 103285. doi:10.1016/j.fbio.2023.103285
26. Yang T, Chen X, Mei Z, et al. An Integrated Analysis of Network Pharmacology and Experimental Validation to Reveal the Mechanism of Chinese Medicine Formula Naotaiyang in Treating Cerebral Ischemia-Reperfusion Injury. *Drug Des Devel Ther*. 2021;15:3783–3808. doi:10.2147/DDDT.S328837
27. Wang KJ, Zhang WQ, Liu JJ, Cui Y, Cui JZ. Piceatannol protects against cerebral ischemia/reperfusion-induced apoptosis and oxidative stress via the Sirt1/FoxO1 signaling pathway. *Mol Med Rep*. 2020a;22(6):5399–5411. doi:10.3892/mmr.2020.11618
28. Cheng X, Yang YL, Li WH, Liu M, Wang YH, Du GH. Cerebral ischemia-reperfusion aggravated cerebral infarction injury and possible differential genes identified by RNA-Seq in rats. *Brain Res Bull*. 2020;156:33–42. doi:10.1016/j.brainresbull.2019.12.014
29. Wang W, Wang Y, Guo Q, et al. Valerian essential oil for treating insomnia via the serotonergic synapse pathway. *Frontiers in Nutrition*. 2022;9:927434. doi:10.3389/fnut.2022.927434

30. Wahid M, Saqib F, Akhtar S, Ali A, Tallei TE, Simal-Gandara J. Mechanistic insights of Cucumis melo L. seeds for gastrointestinal muscle spasms through calcium signaling pathway-related gene regulation networks in WGCNA and in vitro, in vivo studies. *Comput Biol Med.* 2023;155:106596. doi:10.1016/j.combiomed.2023.106596
31. Lv W, Jiang J, Xu Y, et al. Re-Exploring the Inflammation-Related Core Genes and Modules in Cerebral Ischemia. *Mol Neurobiol.* 2023;60(6):3439–3451. doi:10.1007/s12035-023-03275-1
32. Zhou P et al. (2024). Spike lavender essential oil attenuates hyperuricemia and induced renal injury by modulating the TLR4/NF-κB/NLRP3 signalling pathway. *Arabian Journal of Chemistry*, 17(9), 105897. doi:10.1016/j.arabjc.2024.105897
33. Cheng J, Zhang S, Fan A, et al. An immune-related gene signature for the prognosis of human bladder cancer based on WGCNA. *Comput Biol Med.* 2022;151:106186. doi:10.1016/j.combiomed.2022.106186
34. Pei H, Du R, He Z, et al. Protection of a novel velvet antler polypeptide PNP1 against cerebral ischemia-reperfusion injury. *Int J Biol Macromol.* 2023;247:125815. doi:10.1016/j.ijbiomac.2023.125815
35. Wang Y, Xiao G, He S, et al. Protection against acute cerebral ischemia/reperfusion injury by QiShenYiQi via neuroinflammatory network mobilization. *Biomed Pharmacoth.* 2020b;125:109945. doi:10.1016/j.biopha.2020.109945
36. Zhang L, Yuan W, Kong X, Zhang B. Teneligliptin protects against ischemia/reperfusion-induced endothelial permeability in vivo and in vitro. *RSC Adv.* 2020;10(7):3765–3774. doi:10.1039/C9RA08810E
37. Chen X, Li P, Huang R, Zhang J, Ouyang X, Tan D. Ulinastatin affects focal cerebral ischemia–reperfusion injury via SOCS1 –mediated JAK2/STAT3 signalling pathway. *Clin Exp Pharmacol Physiol.* 2023;50(1):107–116. doi:10.1111/1440-1681.13731
38. Zhu T, Wang L, Wang LP, Wan Q. Therapeutic targets of neuroprotection and neurorestoration in ischemic stroke: applications for natural compounds from medicinal herbs. *Biomed Pharmacoth.* 2022;148:112719. doi:10.1016/j.biopha.2022.112719
39. Zhu YL, Huang J, Chen XY, et al. Senkyunolide I alleviates renal Ischemia-Reperfusion injury by inhibiting oxidative stress, endoplasmic reticulum stress and apoptosis. *Int Immunopharmacol.* 2022b;102:108393. doi:10.1016/j.intimp.2021.108393
40. Gao XJ, Xie GN, Liu L, Fu ZJ, Zhang ZW, Teng LZ. Sesamol attenuates oxidative stress, apoptosis and inflammation in focal cerebral ischemia/reperfusion injury. *Exp Ther Med.* 2017;14(1):841–847. doi:10.3892/etm.2017.4550
41. Abalenikhina YV, Py M, AV Shchul'kin, Chernykh IV, Yakusheva EN. Regulation and Role of Hypoxia-Induced Factor 1α (HIF1α) under Conditions of Endogenous Oxidative Stress In Vitro. *Bull Exp Biol Med.* 2022;173:312–316.
42. Pan Z, Ma G, Kong L, Du G. Hypoxia-inducible factor-1: regulatory mechanisms and drug development in stroke. *Pharmacol Res.* 2021;170:105742. doi:10.1016/j.phrs.2021.105742
43. Simon MC. Coming up for air: HIF-1 and mitochondrial oxygen consumption. *Cell Metab.* 2006;3(3):150–151. doi:10.1016/j.cmet.2006.02.007
44. Semenza GL. Hypoxia-inducible factor 1: regulator of mitochondrial metabolism and mediator of ischemic preconditioning. *BBA.* 2011;1813(7):1263–1268. doi:10.1016/j.bbamcr.2010.08.006
45. Cao JW, Tang ZB, Song JH, Yao JL, Sheng XM, Su ZQ. HIF-1α protects PC12 cells from OGD/R-induced cell injury by regulating autophagy flux through the miR-20a-5p/KIF5A axis. *Acta Neurobiol Experiment.* 2022;82(3):358–372. doi:10.55782/ane-2022-034
46. Gong G, Hu L, Liu Y, et al. Upregulation of HIF1α protein induces mitochondrial autophagy in primary cortical cell cultures through the inhibition of the mTOR pathway. *Int J Mol Med.* 2014;34(4):1133–1140. doi:10.3892/ijmm.2014.1850
47. Wu L, Xiong X, Wu X, et al. Targeting Oxidative Stress and Inflammation to Prevent Ischemia-Reperfusion Injury. *Front Mol Neurosci.* 2020;13:28. doi:10.3389/fnmol.2020.00028
48. Warrington JP, Drummond HA, Granger JP, Ryan MJ. Placental ischemia-induced increases in brain water content and cerebrovascular permeability: role of TNF-α. *Am J Physiol Regulatory Integr Comp Physiol.* 2015;309:R1425–1431.
49. Xu X, Piao HN, Aosai F, et al. Arctigenin protects against depression by inhibiting microglial activation and neuroinflammation via HMGB1/TLR4/NF-κB and TNF-α/TNFR1/NF-κB pathways. *Br J Pharmacol.* 2020b;177(22):5224–5245. doi:10.1111/bph.15261
50. Li PL, Zhai W XX, Zhu J, et al. Two Ferulic Acid Derivatives Inhibit Neuroinflammatory Response in Human HMC3 Microglial Cells via NF-κB Signaling Pathway. *Molecules.* 2023;29(1):28. doi:10.3390/molecules29010028
51. Wen S, Unuma K, Funakoshi T, Aki T, Uemura K. Cocaine induces vascular smooth muscle cells proliferation via DRP1-mediated mitochondrial fission and PI3K/HIF1α signaling. *Biochem Biophys Res Commun.* 2023;676:30–35. doi:10.1016/j.bbrc.2023.07.020
52. Zhang B, Gao M, Shen J, He D. Inhaled Methane Protects Rats Against Neurological Dysfunction Induced by Cerebral Ischemia and Reperfusion Injury: PI3K/Akt/HO-1 Pathway Involved. *Archiv Med Res.* 2017;48(6):520–525. doi:10.1016/j.arcmed.2018.01.001
53. Abdel-Latif RG, Rifaai RA, Amin EF. Empagliflozin alleviates neuronal apoptosis induced by cerebral ischemia/reperfusion injury through HIF1α/VEGF signaling pathway. *Arch. Pharmacol Res.* 2020;43(5):514–525. doi:10.1007/s12272-020-01237-y